8-1-2022

Evaluating the Effects of Thermal Cycling on Bone (Cold-Blooded vs Warm-Blooded)

Parker Reed Brewster

EVALUATING THE EFFECTS OF THERMAL CYCLING ON BONE (COLD-BLOODED VS WARM-BLOODED)

A Thesis
presented in partial fulfillment of requirements
for the degree of Master of Science
in the Department of Engineering
at the University of Mississippi

by

PARKER R. BREWSTER

August 2022

ABSTRACT

Thermal cycling, a global threat that is increasingly becoming more real, is a stressing event that can drastically change material properties. Thermal cycling can be used for material strengthening and optimization, but more often than that, thermal cycling is a nuisance that weakens the integrity of structures and coatings. To understand and build better designs that resist the effects of thermal cycling, we look to nature. Though warm-blooded animals regulate their body temperatures within an exceptionally tight range, cold-blooded animals experience relatively extreme temperature fluctuations, and oftentimes, in less than a 5-hour time period. In other words, cold-blooded animals experience significant thermal cycling over the course of their lifetime, whereas warm-blooded animals experience very little or no thermal cycling (internally) over the course of their lifetimes. Through the use of resonant ultrasound spectroscopy, samples of bone from both cold-blooded and warm-blooded species were observed before and after a month-long thermal cycling subjugation. The resonant ultrasound spectroscopy analysis allowed the observation and quantification of any deviations in the elastic makeup of a given bone sample. Results suggested with high confidence that warm-blooded animals underwent significant changes in their elastic makeup as a result of thermal cycling, whereas cold-blooded animals showed either insignificant or no change in their elastic makeup.

ACKNOWLEDGEMENTS

Most notably, of course, I would like to acknowledge the contributions and support provided by my advisor, Dr. Farhad Farzbod. Through his tutelage and expertise, I was able to grow into an extremely efficacious engineer. I would also like to thank my committee members, Dr. Yiwei Han and Dr. Tyrus McCarty. Finally, I would like to acknowledge Matt Lowe for his help with machining and cutting, Dr. Stoddard for his insight into the defense of a thesis, and Tereza Janatová for her various contributions.

TABLE OF CONTENTS

ABSTRACT……ii

ACKNOWLEDGEMENTS……...iii

TABLE OF CONTENTS…….……...iv

LIST OF TABLES…….……vi

LIST OF FIGURES…….……...…...vii

CHAPTER 1: INTRODUCTION……..…...1

1.1 COLD-BLOODED vs WARM-BLOODED

1.2 BONE: PROPERTIES AND COMPOSITION

1.3 RUS

1.3.1 HISTORY AND VALUE: GENERALLY

1.3.2 VALUE IN THE BIOMEDICAL SPACE (RELEVANT RESEARCH)

1.4 EXPERIMENTAL SETUP

1.5 APPLICATIONS / FUTURE STUDIES

CHAPTER 2: THERMAL CYCLING……..……14

2.1 THERMAL CYCLING: A RELEVANT LITERATURE REVIEW

2.2 MATERIALS / MACHINERY

2.3 ENVIRONMENTAL CONDITIONS (STANDARD vs POLARIZED)

CHAPTER 3: RUS ANALYSIS……21

3.1 TRADITIONAL RUS METHODOLOGY

3.2 SAMPLE PREPARATION

3.3 DATA ACQUISITION

3.4 CONTROLS

3.5 RESULTS

3.6 CHARACTERIZATION OF RESULTS

3.7 STATISTICAL ANALYSIS

CHAPTER 4: CONCLUSIONS…….38

4.1 NOTE ON EXPERIMENTAL FINDINGS

4.2 FUTURE DIRECTIONS AND ADJUSTMENTS

REFERENCES…….....41

APPENDIX……44

VITA……...……...59

LIST OF TABLES

Table 1: Experimental Sample Composition.....10

Table 2: Thermal Cycling Protocol.....11

Table 3: Thermal Cycling Protocol.....18

Table 4: Design-Expert Input Table Showing Features and Responses.....31

Table 5: ANOVA for Factor B's Effect on Response 1.....33

Table 6: ANOVA for Factor B's Effect on Response 2.....35

Table 7: ANOVA for Factor B's Effect on Response 3.....37

LIST OF FIGURES

Figure 1: Thermal Regulation....3

Figure 2: Bone Composition Across Species....5

Figure 3: Rus Acquisition and Output Plot....6

Figure 4: RUS Geometries....7

Figure 5: Thermal Cycling Example (Temperature-Sensitive Organics)....14

Figure 6: Specimen Preparation for In Vitro Dentin Bond Durability Test....16

Figure 7: RapidTherm Thermal Chamber....18

Figure 8: Natural Frequencies and Amplitudes....21

Figure 9: Rus Diagram....23

Figure 10: Sawed Disc Ready for Coring....24

Figure 11: Sample Between Two Transducers....25

Figure 12: Excitation Frequencies Across Species....28

Figure 13: Step 1 of MATLAB Protocol: Peak Identification....29

Figure 14: Step 3 of MATLAB Protocol: Midpoint Output....30

Figure 15: Half-Normal Plot for Response 1: 'Shift'....32

Figure 16: One Factor Plot for Response 1: 'Shift'....33

Figure 17: Half-Normal Plot for Response 2: 'Absolute Individual Shift'....34

Figure 18: One Factor Plot for Response 2 35

Figure 19: Half-Normal Plot for Response 3....36

Figure 20: One Factor Plot for Response 3....37

CHAPTER 1: INTRODUCTION

Cold-blooded species can experience extreme internal temperature changes. There have been multiple recorded instances of 55° C temperature changes in less than a 24-hour period. Warm-blooded animals regulate their body temperatures within a tight range. With millions upon millions of years with minimal body temperature regulation, have cold-blooded animals potentially developed a heightened resistance to the effects of thermal cycling? Are the temperature fluctuations simply not polar or rapid enough to induce a material stressing event, or have these animals systematically built a resistance to the effects of thermal cycling? Should the effects of climatic thermal cycling be non-negligible, changes in elasticity would act as a valuable measurable. Resonant ultrasound spectroscopy (RUS) determines or characterizes material properties by measuring resonant vibrations across a given sample. With RUS, it is possible to determine the elastic stiffness of crystalline materials. This chapter will serve as an introduction giving an overview of the theory surrounding RUS, the historical usage of RUS analysis in the biomedical space and otherwise, and the bone properties and composition of both cold-blooded and warm-blooded species. Beyond an introduction to the material, this chapter will briefly look at the potential applications and future studies that could and/or should arise from the results disclosed within this paper. Chapter 2 will look further into thermal cycling. By what mechanisms does it cause stressing events? How was thermal cycling used, and how was it modeled specifically for this experiment? Chapter 3 gives more insight into the RUS protocol (both traditionally and for this study) and the major results, and chapter 4 concludes the thesis.

1.1 COLD-BLOODED vs WARM-BLOODED

It is well known that cold-blooded animals do not maintain constant body temperatures. To acquire heat, cold-blooded animals must look to their environment. Outside of birds and mammals, most animals in the animal kingdom are in fact cold-blooded. Regardless of field or practice, a shockingly high number of phenomena can be explained by understanding the effects of varying surface area to volume ratios. Using size and shape alone, a species' temperature regulation mechanism can be accurately ascertained. Generally speaking, larger animals tend to be warm-blooded. Whales, elephants, buffalo, etc. have extremely low surface area to volume ratios. Their vast volumes and relatively little surface areas ensure inadequacy in terms of efficient external heat transfer. This same principle can be applied to smaller mammals. Smaller warm-blooded animals tend to have tighter height to width ratios. In other words, their surface area to volume ratios are still relatively small. Cold-blooded species tend to have extremely high surface area to volume ratios. Snaked, alligators, lizards, etc. are all long and skinny. This creates as much surface area for heat transfer as possible while maintaining just enough volume to retain bodily function.

So, cold-blooded animals cannot regulate their body temperature. What does that mean? For starters, this means that if it is 100° F outside, every cubic inch of a cold-blooded animal's body will eventually reach 100° F at a minimum. That statement holds true even in 20° F conditions. As alluded to in the introduction, there have been recorded instances of more than 55° C variations in less than a 24-hour period. This means that in less than 24 hours, thousands of species of cold-blooded animals experienced extreme thermal cycling. In 1972, the town of Loma, Montana experienced a temperature spike from -54° F to 49° F. This seemingly extreme case is not necessarily an overwhelming outlier in terms of environmental

thermal cycling. The Sahara desert regularly cycles between 40 and 100° F. Cobras, crocodiles, frogs, toads, lizards, chameleons, etc. can all call the Sahara Desert their home. For many thousands of years, these species have endured extreme thermal cycling. In contrast, there are mammals living in sub-zero climates that maintain a strict 37° C body temperature year-round.

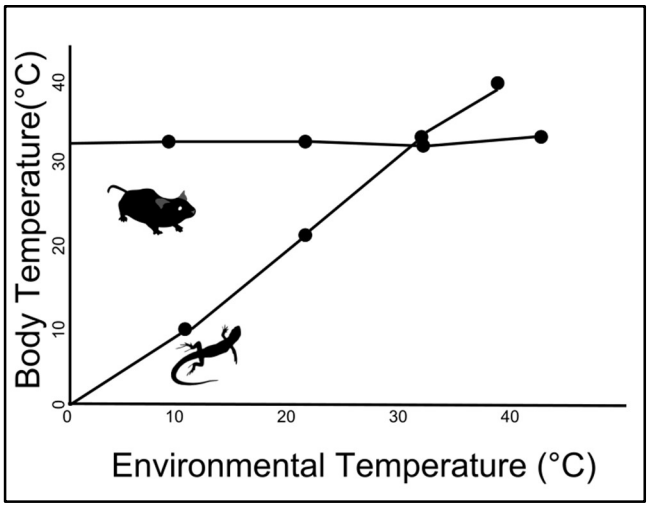

FIGURE 1: THERMAL REGULATION[22]

How do warm-blooded animals maintain such a tight range of acceptable body temperatures? Given the optimum biological temperature of 37° C, most warm-blooded animals are constantly fighting to raise their body temperature. Doing so requires an immense amount of energy. Mass per mass, warm-blooded animals consume significantly more food. For warm-blooded animals, heat lost is proportional to body surface area, and heat produced is proportional to body mass. This translates to a positive correlation between body size and the ability to maintain stable temperatures more easily. In contrast, cold-blooded animals drive their metabolism using their surroundings. Some reptiles can go an entire year without a single meal. There are clear advantages and disadvantages at play here. Notably, cold-

blooded animals cannot function in low temperatures: the lower the temperature, the slower the metabolism and needed chemical reactions.[1]

Evolutionarily, warm-blooded animals have developed a vast library of tools to maintain their body temperatures. These animals have selectively created insulation, intelligent blood vessel alignment, rapid metabolism, wool, etc. for warming up the body, and sweat glands, dry breathing, etc. for cooling down the body. We know that thermal cycling can wreak havoc on material properties (hardness, elasticity, porosity, etc.). Given that cold-blooded animals have had millions upon millions of years to combat the effects of this thermal cycling, what tools have they created in their defense?

1.2 BONE: PROPERTIES AND COMPOSITION

To understand the properties and composition of bone, it is important to consider mineral phase, organic phase, other minerals, and water content. Bone consists of hydroxyapatite, type I collagen, non-collagenous proteins, lipids, and water. The relative amount of each constituent, and the matrix itself, can greatly alter the mechanical properties of bone. Comparing cold-blooded species to warm-blooded species in terms of their bone composition reveals a distinct difference. Warm-blooded animals have more mineral-dominant compositions and cold-blooded animals have more water and/or organic-based compositions.[2]

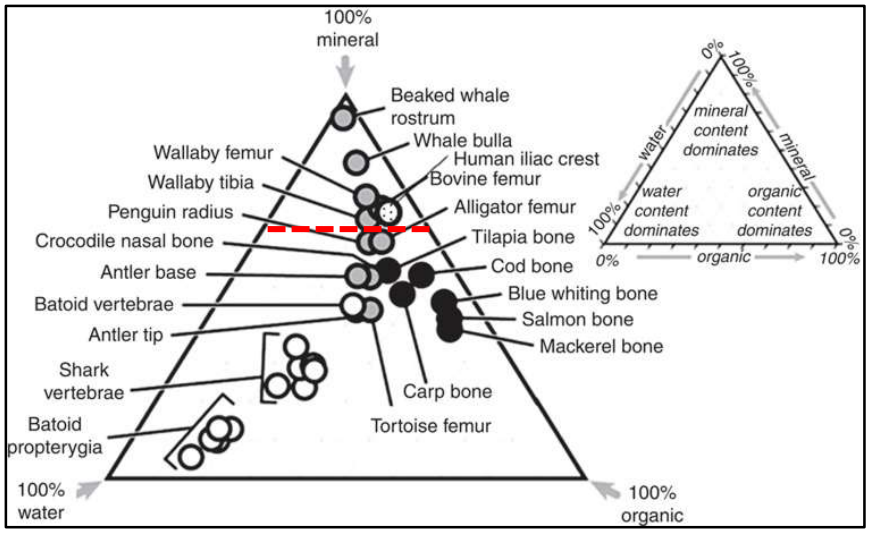

FIGURE 2: BONE COMPOSITION ACROSS SPECIES[2]
Note: Dotted red line delineates the boundary between cold and warm-blooded (w/ penguin as the sole exception)

"There is a clear difference in bone structure between modern cold-blooded and warm-blooded animals. Warm-blooded animals tend to have highly vascularized bone tissue. Cold-blooded animals, on the other hand, have relatively dense bone, sometimes even showing annual growth rings." – Thomas E. Williamson. There is a hot debate in the paleontology world; were most dinosaurs cold-blooded or warm-blooded? There is evidence to support that they could have been either cold-blooded, warm-blooded, or a mix of the two. Growth lines within dinosaur bones first suggested that they were cold-blooded species. However, a study on a vast number of ruminants (ungulate, cud-chewing mammals) revealed growth lines much like those found in dinosaur fossils.[3] In truth, most paleontologists are starting to accept that dinosaurs were likely some hybrid between cold-blooded and warm-blooded. If studying the effects of thermal cycling on bone samples proves to be a viable tool in the distinction between cold-blooded and warm-blooded animals, this could change the way we approach dinosaur characterization.1.3

RESONANT ULTRASOUND SPECTROSCOPY

Resonant ultrasound spectroscopy (RUS) takes advantage of objects having natural frequencies at which they vibrate when excited. The frequency at which these excitations occur depends largely upon three factors: elasticity, size, and shape. Knowing a sample's size and shape, and by determining those excitatory frequencies, RUS is capable of back-calculating the elastic tensor of a given sample.

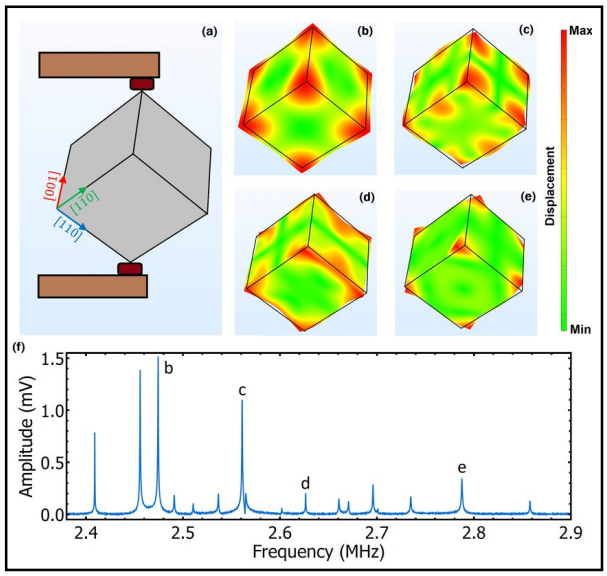

FIGURE 3: RUS ACQUISITION AND OUTPUT PLOT[23]

1.3.1 HISTORY AND VALUE

RUS has a complex history and evolution. Using resonance as a means to determine a material's elastic properties has been practiced since the 1920s. Over the course of the next 100 years, many of the advancements revolved around increasing the scope of allowable or testable geometries (cylindrical, spherical, and finally rectangular parallelepipeds).[4] For many instances, the rectangular parallelepiped shape discovered in the 1960s is still the superior sample shape for RUS.[5]

Traditional RUS was largely developed and first published in 1993. This introduced a RUS acquisition and analysis protocol that allowed the measurement of a material's elastic moduli.[6]

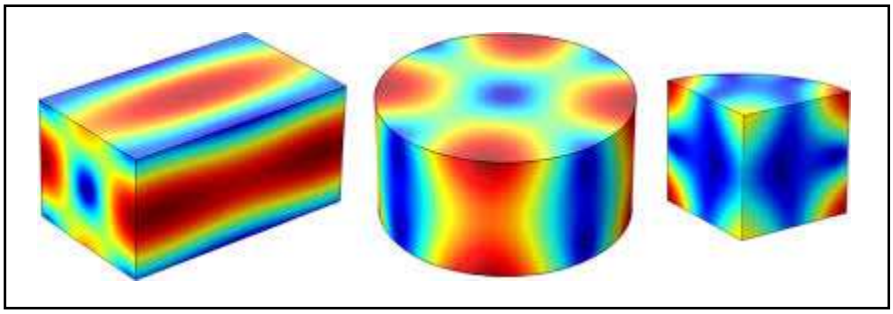

FIGURE 4: RUS GEOMETRIES[24]

RUS methods continue to improve and adapt. Contactless resonant ultrasound methods have been developed that allow the measurement of elastic constants of human dentin and bone in situ.[7] RUS has also now been optimized for high-temperature environments.[8] Beyond simple optimizations, an entirely new means of RUS was recently developed. In 2008, a laser-based technique used lasers for both excitation and response measurement.

1.3.2 VALUE IN THE BIOMEDICAL SPACE

This section acts as a research summary of papers using RUS in biomedical applications. Each one of the following papers was used to inform the experimental design process.

One study by Cai x. et al investigated the anisotropic elastic properties of human cortical bone using resonant ultrasound spectroscopy. The claim was that though nanoindentation can be used to characterize a sample's elastic properties, it can hardly reveal elastic anisotropy. They proposed a method by which millimeter-sized bone samples were measured with RUS technique and the Fast Fourier Transform homogenization method. To their knowledge, they

were the first group to discover the whole set of the EVM stiffness tensor on the same specimen with a large number of samples. They largely felt that their methods were highly precise, but not necessarily accurate. They believed that the significance of their paper was that its results and proposed methodology could be used to develop a better understanding of bone mechanics and biological phenomena (such as mechanotransduction).[9]

A different study assessed trabecular bone elasticity with RUS methods. In doing so, they believed they would contribute to a better understanding and/or methodology for the determination of bone tissue elasticity (an important analysis for the clinical assessment of bone strength). Methodologically, they measured the first mechanical resonance frequency of a freestanding cuboid sample, and then used that to back-calculate elastic modulus. To simply say 'back-calculate' is a gross over-simplification. This requires the computation of the apparent stiffness tensors via micro-finite elements for a set of theoretical values of Young's modulus. Finally, the elastic modulus was determined by interpolation using resonance frequencies and the modeled free-vibration resonance frequencies.[10]

In an experiment conducted by Lee T. et al, RUS was used for the evaluation of bovine bone. As a control, the results were compared to data obtained with the traditional wave transmission ultrasound method. This paper was valuable in shedding light on the way in which we needed to approach this project. The paper reinforced the idea that though some low-damping materials required just a single measurement to yield sufficient resonant frequencies to determine all of the anisotropic elastic constants, bone is not one of such materials. At ultrasonic frequencies, bone has relatively high viscoelastic damping, and so resonant peaks tend to have significant overlap. As a result, more than one measurement is

required (several in fact), and even then, it is not likely that all elastic constants will be found.[11]

A study by Semaan M. et al assessed the elastic coefficients of child cortical bone using RUS. The sample size was exceptionally small (just 7 fibulae), but they believe that the results were consistent with the hypothesis and/or known values. The claim is that the assessment of these anisotropic elastic properties of non-pathological child cortical bone is an important challenge to overcome in the clinical setting.[12]

In 2017, Cai X. et al sought to quantify stiffness measurement errors in RUS via analysis of human cortical bone. This paper was most influential in informing the decision for the proposed metrics by which the bone samples would be compared against each other. Research suggests that, in order to obtain accurate stiffness constants and engineering moduli, bone samples have to have near-perfect geometries and post-processing (surface regularity). For larger sample sizes, this becomes not only tedious, but impossible.[13]

In a study conducted by Zapata et al., 42 cylindrical alligator bone samples were obtained from the facial bones of 4 fresh alligator mandibles. In terms of the samples' material properties (specifically their elastic properties), these samples were found to be extremely similar to samples from mammalian long bones. However, the properties were fairly different when compared to mammalian facial bones. They claim that these results directly disprove the theory that the high bone strain magnitudes recorded from alligator mandibles (in vivo) are attributable to a lower stiffness of alligator mandibular bone.[14]

1.4 EXPERIMENTAL SETUP

To conduct resonant ultrasound spectroscopy, the bone samples needed to have sufficient volume. Beyond the volumetric constraints, the samples needed to be entirely either compact or spongy bone. Given those two constraints, the list of viable species was significantly shortened. Ultimately, three species were analyzed: alligator (cold-blooded), horse (warm-blooded), and cow (warm-blooded). In total, there were 29 samples under observation. The following table illustrates the makeup of the samples.

TABLE 1: EXPERIMENTAL SAMPLE COMPOSITION

	Species	**# of Individuals**	**# of Samples**
Femur	Cow	3	6 compact
	Horse	1	3 compact
	Alligator	3	4 compact, 2 spongey
Humerus	Cow	1	2 compact
	Horse	1	2 compact
	Alligator	3	6 compact, 4 spongey

To prepare the samples that would undergo RUS, a handsaw was used to cut discs throughout the length of the long bones. From those discs, samples were cored out of either compact or spongy bone using a slow-speed, diamond-tipped, hollow core drill bit (6 mm ID). All 29 samples were cored from anatomically comparable regions across all three species. Following the coring, all samples were sanded with a slow, constant speed, and frequently changed, high grit sanding discs. This sanding was done to produce samples that were comparable in length and uniformity. Once the uniform samples were produced, one

planar side of each device was marked with a black notch. They were then imaged with a low magnification microscope. Those images were taken at both planar ends of every sample. The samples were then weighed and measured using high-resolution calipers. Preliminary RUS readings were taken using a resonant ultrasound spectrometer developed by Alamo Creek Engineering. The samples were then systematically placed on the black notched side and equidistant from one another within a thermal chamber. This thermal chamber was then programmed to cycle with the following steps.

TABLE 2: THERMAL CYCLING PROTOCOL

Step #	Step Type	Step Time	Setpoint (DegC)	Thermal Boost	Deg/min
1	Ramp Time	00:01:00	25	10	0
2	Ramp Time	00:05:00	0	10	5
3	Soak	00:10:00	n/a	n/a	n/a
4	Ramp Time	00:04:00	40	n/a	10
5	Soak	00:10:00	n/a	n/a	n/a
6	Loop	n/a	n/a	n/a	n/a
7	EOP	n/a	n/a	n/a	n/a

The program was created to loop a total of 1400 cycles (approximately a 29-day period with a 0-40 degC thermal cycle). The specifics will be discussed in a later section. Once the thermal cycling was complete, all samples were carefully removed, imaged, weighed, and measured again. Each sample was then measured again using RUS (signal sent through a drive transducer, through the sample, into the pickup transducer, and displayed as a spectrum). The samples were reoriented so that measurements were taken four times on both the marked and unmarked sides of the cylinder. All relevant data were collected and then

exported to excel where further data organization was performed. The newly cleaned data was then exported to MATLAB for the characterization and quantification of frequency shifts that may or may not have happened. All quantifiable responses were imported into a statistical analysis package (Design Expert), and the factorial significance was discovered/characterized.

1.5 APPLICATIONS / FUTURE STUDIES

Should a particular species or set of species demonstrate a heightened resistance to the negative effects of thermal cycling, the next logical step would be to systematically determine why or how that resistance came to be. Whether the resistance arises from changes in elemental composition, lattice frameworks, vascularity, density, or otherwise, understanding the mechanisms by which this resistance came to fruition could be exceptionally useful in optimizing a vast array of fields and/or efforts.

In the realm of biomechanics, these findings could be used to optimize the design of implants, prosthetics, and space/aqua suits to be better adapted for thermal cycling. For example, the human mouth can undergo fairly extensive thermal cycling. To increase average lifespans, dental implants and caps could be further optimized at the front end to better resist the stresses arising from years of thermal cycling.

These findings could also have potential in the world of biomedical engineering and drug delivery. If one species or group of species (cold-blooded animals for instance) were to show advanced resistance to thermal cycling, mimics could be developed to increase the structural performance of human bone. Osteoporosis and bone cancer have obvious points of potential improvement, but with credible claims and warnings of global temperature polarization having become more and more prevalent, there could also soon be a market or need for the

improvement of resistance to thermal cycling (human bone). Though humans are warm-blooded and can in fact regulate their body temperatures, rapid fluctuation in temperatures is still a stressing event that would only be made worse if global temperature polarization does indeed come to fruition.

Perhaps the most obvious fields with potential room for thermal cycling optimization would be industrial/mechanical and civil engineering. Cheaper building materials that could withstand extreme temperature conditions, high power and/or friction machinery requiring cooling systems, wire coatings, satellite and spacecraft components, etc. all have room for significant improvement in terms of thermal cycling resistance. In fact, with LEO satellites experiencing thermal cycling between -150 and 150 degC, it is not hard to understand why it is believed that thermal cycling is their number one mechanism of failure.[15]

In a later section, both improvements to be made and future studies will be discussed in greater detail. Perhaps most importantly, it is believed that at least one more controls should be added in order to more confidently confirm the following hypothesis: **"Have cold-blooded animals developed a resistance to thermal cycling?".**

CHAPTER 2: THERMAL CYCLING

Thermal cycling is not inherently negative. In fact, some alloys are heat-treated via thermal cycling to strengthen mechanical properties and improve ductility.[16] That having been said, thermal cycling is more often a nuisance that does or can affect almost every engineering discipline. How is it that one process could affect different materials in such vastly different ways? Thermal cycling is a stressing event that causes a material or sample to experience molecular reorganization. In some materials and in a controlled setting, that 'molecular reorganization' can result in the tightening or optimization of the material's particulate structure, thus relieving stress and minimizing fracture points.[17] In most materials, that same molecular reorganization wreaks havoc on the system by introducing voids, disorder, stress points, elongated fissures, etc. Thermal stress arises from a material's tendency to expand with increases in heat. When a material is rapidly cooled and heated, different zones of that material expand and contract at different rates and degrees. At some point within that cycle, the material will surpass its elastic limit where each expansion and contraction results in a permanent change.

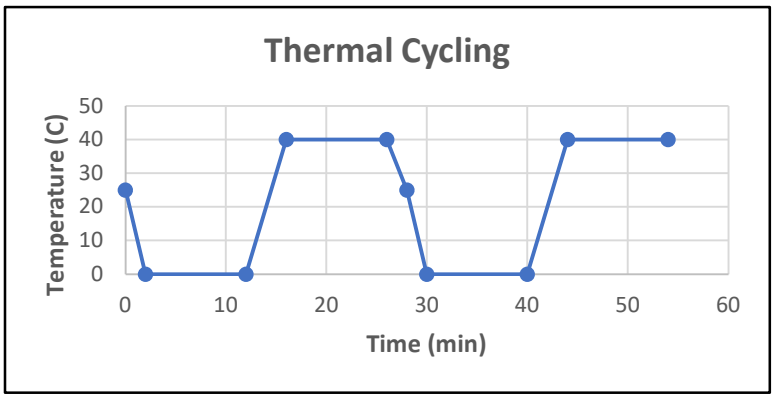

FIGURE 5: THERMAL CYCLING EXAMPLE (TEMPERATURE-SENSITIVE ORGANICS)

2.1 THERMAL CYCLING: A RELEVANT LITERATURE REVIEW

Most studies relating human biology to thermal cycling have to do with dentin. With humans being warm-blooded, there are few justifications for the research of thermal cycling and its effect on various biological processes or systems. One exception to that rule is the mouth. If you were to sip on coffee and enjoy a nice ice cream, your mouth could potentially cycle between 0° C and 85° C exposures. Many of the studies looking at thermal cycling as it relates to the mouth look at the effects of thermal stress on bonding systems (dental 'glues').

One study by Miyazaki M., Sato M., and Onose H et al. looked specifically at 2-step dental bonding systems. In this study, they were comparing commercial products against each other. To do so, they divided the samples into 4 different groups: (a) stored in 37° C water for 24 hours, stored in 37° C water for 24 hours followed by subjection to thermal cycling between 5° C and 60° C for (b) 3,000 cycles, (c) 10,000 cycles, and (d) 30,000 cycles. The measurable response for this study was shear testing, not resonant ultrasound spectroscopy, but their methods and controls were used to inform the decision-making process in the design of this experiment on bone samples.[18]

A similar study by T. Nikaido et al. also looked at the effects of thermal cycling on dentin and various bonding agents. In this study, they were characterizing the in vitro durability and fracture modes via micro-tensile bond strength testing. With the two most recently discussed papers both using water baths as the mode of thermal cycling, it is believed that the addition of a water bath thermal cycle would make a valuable addition to this experiment's protocol.[19]

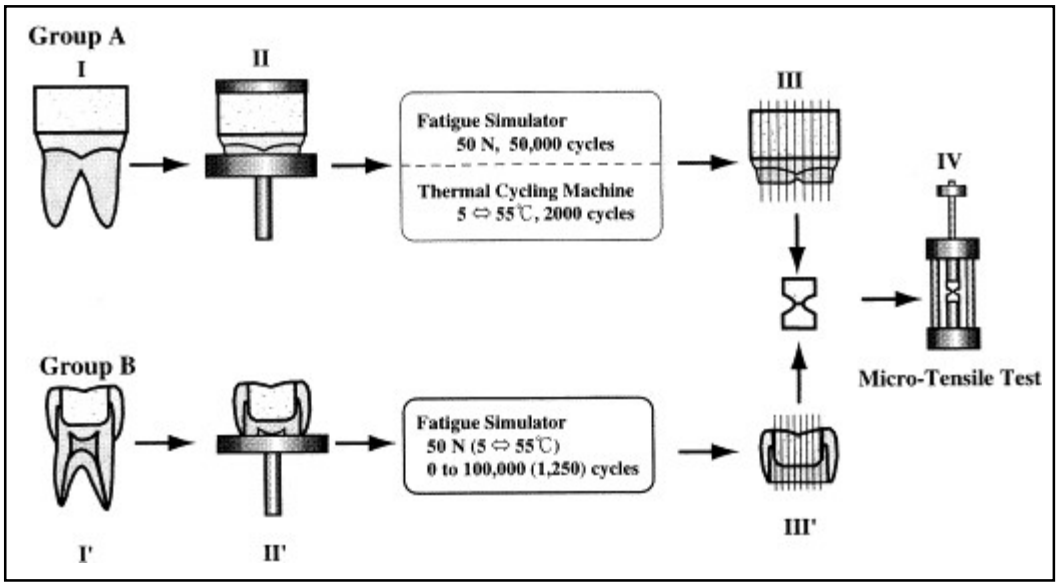

FIGURE 6: SPECIMEN PREPARATION FOR IN VITRO DENTIN BOND DURABILITY TEST[19]

Perhaps the most enlightening paper in terms of thermal cycling and its effects would be a paper by S. Agbadua et al. entitled "Thermal Cycling Effects on the Fatigue Behavior of Low Carbon Steel". This paper discusses thermal cycling as a conglomeration of two distinctly different modus operandi: low-frequency thermal cycling and high-frequency thermal cycling. In essence, there are two tunable dials when discussing thermal cycling: temperature and time. Time can of course be broken down further in ramp and steep / soak times, but it all condenses down to temperature and time. To produce an effect, thermal cycling could use extremely polar temperatures with relatively long ramp and soak times, or on the other side of the spectrum, it could use relatively non-polar temperatures with extremely brief/quick ramp and steep times. Though this is a gross simplification, stating it does have merit: polar temperatures with long ramp and soak times will generally produce larger imperfections (cracks, voids, fault planes), however, non-polar temperatures with quick ramp and soak times will produce higher

quantities of imperfections. As a result, designing a thermal cycling protocol largely depends on what the measurable response will be. Larger imperfections result in more predictable failures at specific locations, but characterizing the integrity of a sample in its entirety would be more difficult. Was one of the links of the chains damaged severely, or were all the links damaged moderately?[17]

2.2 MATERIALS AND METHODS

For the thermal cycling conducted in this experiment, a RapidTherm® thermal chamber with an IDEC touchscreen controller was used. This particular chamber is capable of cycling between -75° C and 200° C. The following information is from RapidTherm's® provided instruction manual. The controller uses a cascaded control strategy of two temperature channels and two temperature sensor inputs to enable the chamber to produce the fastest possible temperature change rates and/or the optimum temperature control of the device under test (DUT).

The controller uses thermalboost to over or under drive the temperature of the air being supplied into the chamber's workspace. The temperature of the air being supplied into the chamber is controlled by setpoint 2 Setpoint 1 is the user-defined value that the DUT is controlled to. Another unique feature of the chamber that promotes high acceleration would be its fan. The chamber's control system utilizes a variable frequency drive to vary the speed of the fan motor(s). This is to automatically provide the highest airflow possible in the chamber in accordance with the varying temperature setpoints of a test. This allows the DUT's temperature to be changed to the new setpoint as quickly as possible.[20]

FIGURE 7: RAPIDTHERM THERMAL CHAMBER[25]

The following table, TABLE 3, depicts the parameters of the thermal cycling subjugation. Samples were adhered to a two-sided tape (to prevent fan disturbance) and placed in a predetermined grid directly on the floor of the thermal chamber. The protocol was then initiated.

TABLE 3: THERMAL CYCLING PROTOCOL

Step #	Step Type	Step Time	Setpoint (DegC)	Thermal Boost	Deg/min
1	Ramp Time	00:01:00	25	10	0
2	Ramp Time	00:05:00	0	10	5
3	Soak	00:10:00	n/a	n/a	n/a
4	Ramp Time	00:04:00	40	n/a	10
5	Soak	00:10:00	n/a	n/a	n/a
6	Loop	n/a	n/a	n/a	n/a
7	EOP	n/a	n/a	n/a	n/a

The first step, Step 1, was a control step to ensure that the starting point was returned to normal temperature (25° C). Step 2 brought the internal temperature down to 0° C over the course of 5 minutes (5 degrees per minute). Step 3 allowed a soak time with a constant 0° C environment. This step was meant to encourage the completion of material contraction. Step 4 ramped the internal temperature from 0° C to 40° C over the course of 4 minutes (10 degrees per minute). Step 5 was another soak step with the same reasoning as Step 3, Step 6 told the protocol to loop back to Step 1 (1400 times), and finally, Step 7 broke the loop and terminated the thermal cycling.

2.3 ENVIRONMENTAL CONDITIONS (STANDARD VS POLARIZED)

The determination of the thermal cycling protocol was a process that was not taken lightly. Many, if not all, of the previously cited research papers went into the decision-making process. The two most significant papers in informing the design of the protocol were those papers entitled “Thermal Cycling Effects on the Fatigue Behavior of Low Carbon Steel” and “Influence of Thermal Cycling on Dentin Bond Strength of Two-step Bonding Systems”.[17,18] Using all of the available resources, it was determined that the protocol seen in the above TABLE 3 would be the most ideal starting point to elicit the potential measurable response.

Though an accelerated model could likely have been implemented, it was decided that a model more closely aligned with nature would produce the most representative results. Recall from the introduction that species native to the Sahara region are frequently subjugated to a thermal cycle ranging from 25° F to 100° F (0° C to 38° C). For that reason, the decision was made to create a protocol that would respect the limitations of nature (0° C to 40° C).Following the determination of the thermal peak and valley, the ramp and soak times had to be

determined. A relatively quick acceleration time was needed to produce a shock response, and the soak time needed to be long enough to allow the sample contraction or expansion to finalize. To maximize the number of cycles possible in the given amount of time, that soak time needed to be as brief as possible. Looking through the literature, it was decided that, for the volume of our organic samples, a 10-minute soak time would be a happy medium. For future studies, an even more aggressive rate could be explored.

CHAPTER 3: RUS ANALYSIS

Resonant ultrasound spectroscopy (RUS) was briefly introduced in the introduction. A sample, in this case cylindrical, is placed between two acoustic transducers. One transducer delivers a swept sinusoid, and the other transducer monitors the resulting vibrational response. Also briefly mentioned in the introduction: a material has natural frequencies at which excitations occur. If the input frequency from the first transducer matches the natural frequency of the sample, the vibrations will be amplified and recorded by the second transducer.

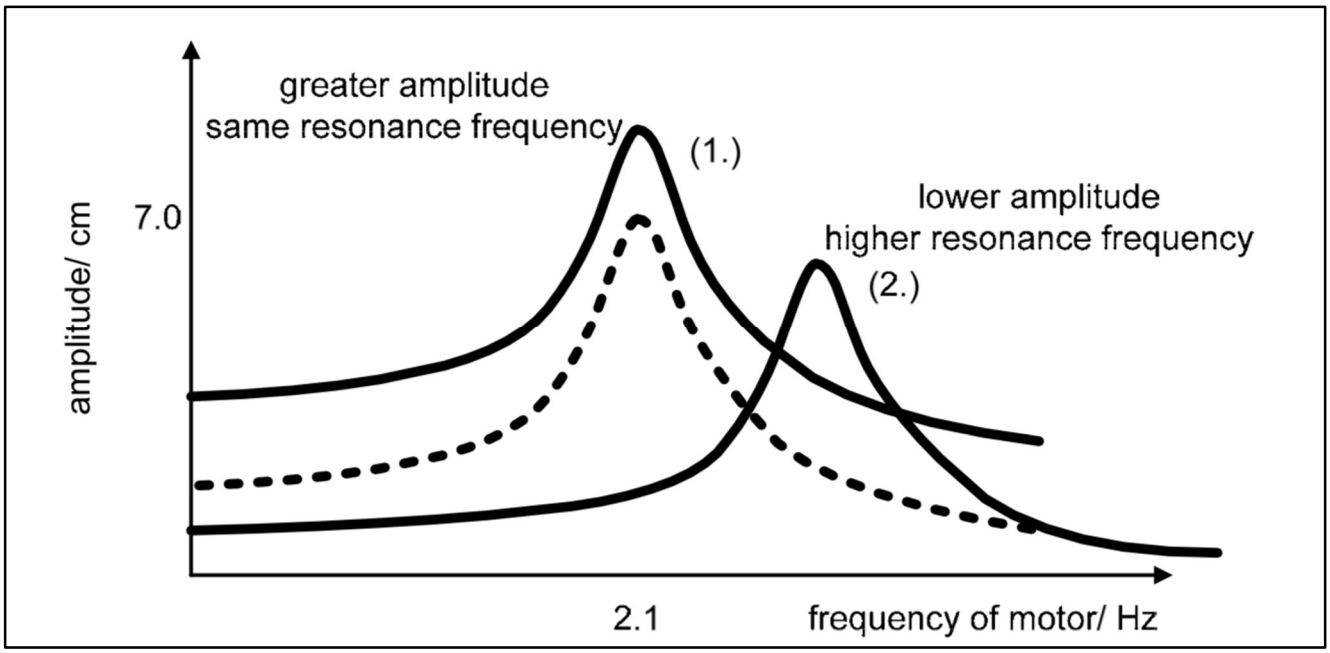

FIGURE 8: NATURAL FREQUENCY AND AMPLITUDES
https://i.stack.imgur.com/aWTcE.png

3.1 TRADITIONAL RUS METHODOLOGY

Traditionally, the protocol for the determination of the elastic tensor via RUS would look something like the following: a custom file with the expected frequency range would be loaded into the data acquisition program, and then the sample would be placed between the two transducers and the aforementioned values (input frequencies and amplitude of the response) would be determined for that particular positioning. Depending on the shape of the sample, n number of sample position readjustments would take place. For example, this lab recently characterized rectangular prisms. To adequately capture each mode (modes can be present in some orientations, but not in others), the rectangular prism had to be characterized edge -> edge and corner -> corner for a total of 10 readings. The output of these readings is a 'Format Resonances' plot with exportable frequency and voltage values. At that point, the user can then decide to either select just the peaks ('modes') for export, or the entire range of values for export. Once exporting the data to CSV, a mode matching and averaging of values is performed. For this, it is assumed that no one position would have a unique mode. The observation of the collective informs the decision on which peaks are actually modes. The resulting list of frequencies (peak frequencies) is then fed back into the software and iterated once through (at this point, another custom file containing the sample's dimensions and mass would need to be uploaded). This generates a new list which includes predicted frequencies (using known literature values as a reference point). Both the experimental and theoretical values would then be fed back into the program and iteratively run until sufficient convergence occurs. The output file would then contain estimations for % error (experimental frequency vs theoretical), bulk modulus (GPa), C values (C11, C22, C33, C23, etc.), and RMS error.

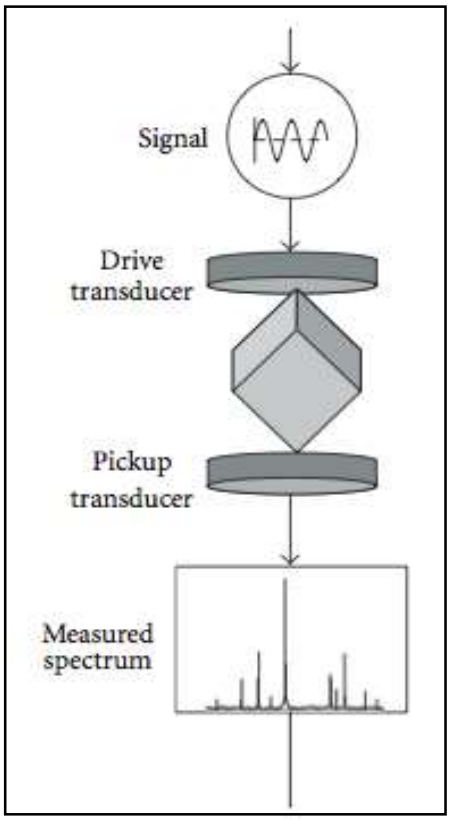

FIGURE 9: RUS DIAGRAM[26]

3.2 SAMPLE PREPARATION

The sample preparation technique was adapted largely by referencing a paper by Kinney J, Gladden J, Marshall G et al.[21] Through referencing this material and others, it was decided that a slow-speed, diamond-tipped drill bit would be most ideal. Humeruses and femurs were cut into approximately 1" thick discs (axially cut). Those discs were then supported by a bench vice while samples were cored using a Jet® drill press and a diamond-tipped, hollow drill bit (6 mm internal diameter). Samples were cored from either spongy or compact bone regions, but never from a combination of the two. Samples were also always cored from anatomically similar regions across all three species.

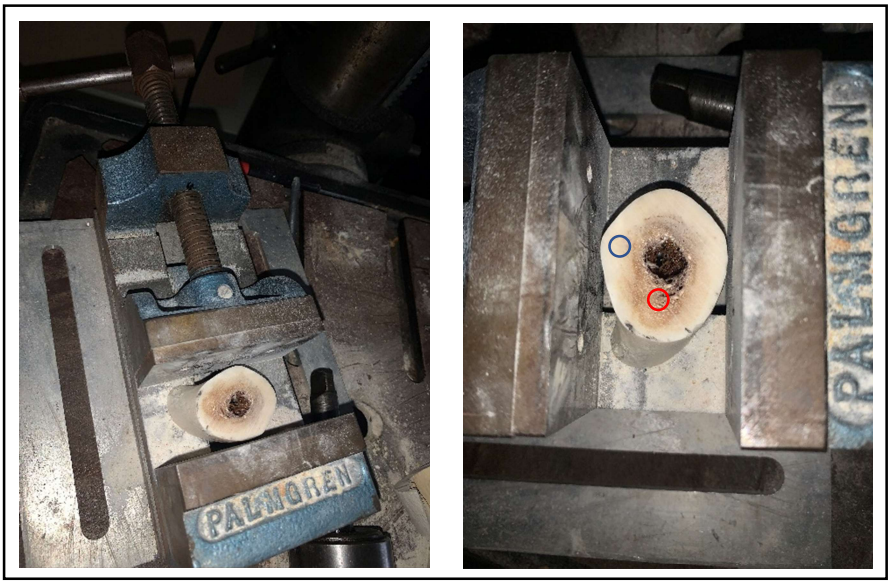

FIGURE 10: SAWED DISC READY FOR CORING

Note: Blue circle indicates compact region, red circle indicates spongy region

Those cored samples were highly uniform in diameter, but not in length. To produce samples with similar lengths and flat caps, a rotary tool was used. Sandpaper discs were used on the lowest RPM to shape the samples into comparable dimensions. After all processing was finished, samples were cleaned with compressed air and stored individidually in air-tight bags. For all remaining measurements and procedures, the samples were handled with gloves and tweezers to prevent oil contamination.

3.3 DATA ACQUISITION

Each of the 29 samples of interest had custom procedures. Once a sample was positioned between the two transducers of the RUS instrument, a configuration file was created. Creating this configuration file takes some trial and error. The start frequency, end frequency, output

amplitude, coarse step, fine step, and step duration can all affect the quality of the output. Once those settings were optimized, the configuration file was saved and was specific to that sample. Following the thermal cycling subjugation, that same configuration file was used for the same sample. This ensured not only similar output quality, but identical frequency ranges and steps. This procedure was replicated across all 29 samples.

Following the creation of the configuration file, each sample was measured edge -> edge. This measurement process populated a spectrum recorder and then generated a plot of peaks with the resonance detector. Those values composing the plot (magnitude – V, and Frequency – Hz) were then exported as a CSV file. Using excel, that data was then cleaned and prepped further. For each sample, the 'edge -> edge' position was then rotated approximately 90 degrees, and the process was repeated. This repetition was done for two more 90-degree rotations, and then the sample was turned over, and that procedure was repeated on the sample's opposite side. The result of those reorientations was 8 reads (Magnitude vs. Frequency) per sample.

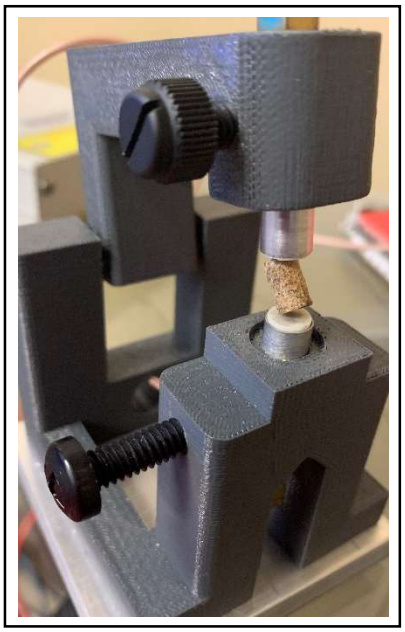

FIGURE 11: SAMPLE BETWEEN TWO TRANSDUCERS

Once all 8 datasets were in excel and cleaned, an average of the magnitudes was computed. This average was saved and assumed to be the new approximation of that sample's excitation frequencies.

3.4 CONTROLS

There were three controls implemented in this procedure. The first 'control' lies within the previously discussed protocol. Taking edge -> edge measurements on both sides of the cylindrical sample created a scenario in which two theoretically identical readings could be averaged together.

More importantly: one sample from each bone from each species was selected at random to be fully characterized twice. In doing this, any observed excitation frequency shifts arising from thermal cycling could be validated by comparing the control against the original reading. Following the thermal cycling, those samples that were randomly selected to have control trials were again fully characterized twice. This, of course, goes to further validate any observed shifts arising from thermal stress.

Finally, two samples from each species (one from humerus and one from femur) were prepared and processed, but never subjugated to thermal cycling. Those 6 samples were measured with the same RUS protocol and 30 days apart. This control was added to ensure that any potential frequency shifts were truly a result of the thermal cycling and not a result of the material relaxing post-processing.

3.5 RESULTS

It has been alluded to throughout the paper, but the final measurable has not been explicitly discussed. Section 3.1 was dedicated to describing traditional RUS analysis protocol because that is, in fact, not the protocol or measurable that was used for this experiment. Certain papers have suggested that, in order to obtain accurate stiffness constants and engineering moduli, bone samples have to have near-perfect geometries and post-processing (surface regularity). For larger sample sizes, this becomes not only tedious, but impossible. 13 Strictly following the aforementioned RUS protocol, it became apparent that accurately defining a material's elastic tensor would be next to impossible. However, the plot of resonance frequencies was extremely precise across control trials. That plot in and of itself can be used as a quasi-quantifier of a sample's elastic character. It was proposed that if, and only if, a sample was being compared against itself, its plot of excitation frequencies would be not only sufficient, but faster and equally as efficacious.

Before revealing the results, it seems prudent to again discuss the abbreviated hypothesis: "Have cold-blooded animals developed a resistance to thermal cycling?". The results and statistics will be discussed in greater detail across the coming sections, but to depict the overall character of the experimental results, the following figure, FIGURE 9, has been provided. The shifts or lack thereof should be apparent, but the steps taken towards quantifying those shifts will be described in the next section, **section 3.6**. This figure depicts the excitation frequencies of samples from the femurs of all three species: alligator, cow, and horse.

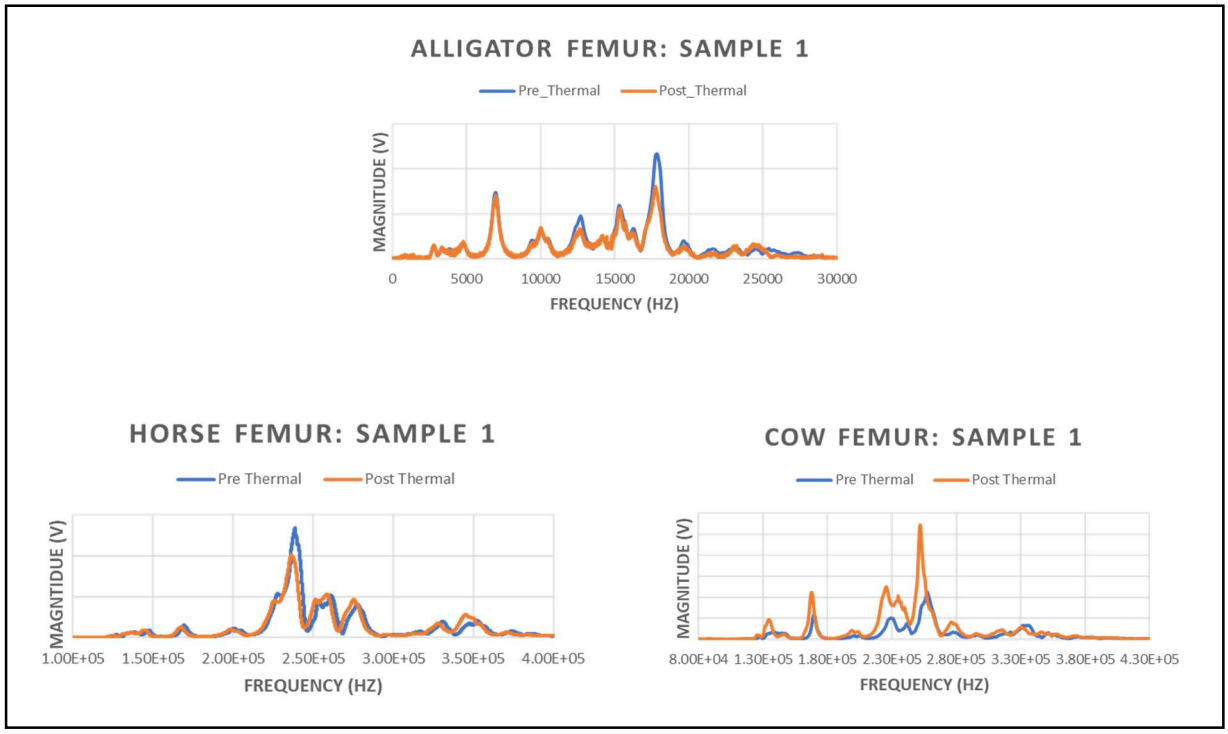

FIGURE 12: EXCITATION FREQUENCIES ACROSS SPECIES
Note: Observe shifts seen across the warm-blooded species but not within the cold-blooded species

3.6 CHARACTERIZATION OF RESULTS

Across all 29 samples, it was immediately obvious that the modes related to the warm-blooded species were shifting more than the modes related to the cold-blooded species. However, a protocol needed to be developed that would take the two plots (Pre Thermal and Post Thermal), and quantify the characteristic shift. To execute this protocol, MATLAB was implemented (code in appendix). This MATLAB code took two inputs (csv files containing the data from both pre-thermal and post-thermal RUS analyses), identified potential peaks of interest, asked the user to choose three peaks, matched the three peaks across both plots (pre and post-thermal), created horizontal line segments at 2/3 the height of each peak, calculated the midpoint of those line segments, and took the difference of those midpoints for all three peaks. Once the three differences were calculated, an average of those three differences could be taken.

That average was then considered to be the new quantifier used to depict the sample's overall shift in excitation frequencies, thus characterizing the sample's change in elastic makeup.

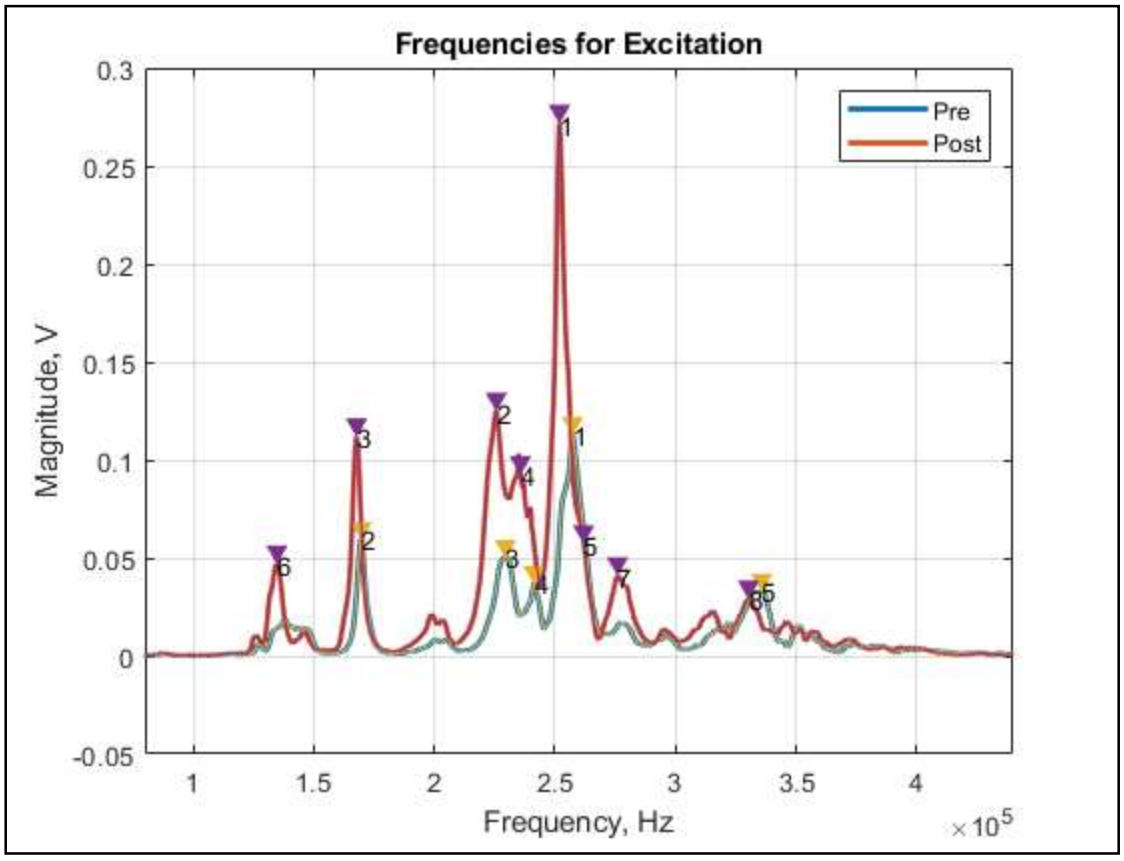

FIGURE 13: STEP 1 OF MATLAB PROTOCOL: PEAK IDENTIFICATION

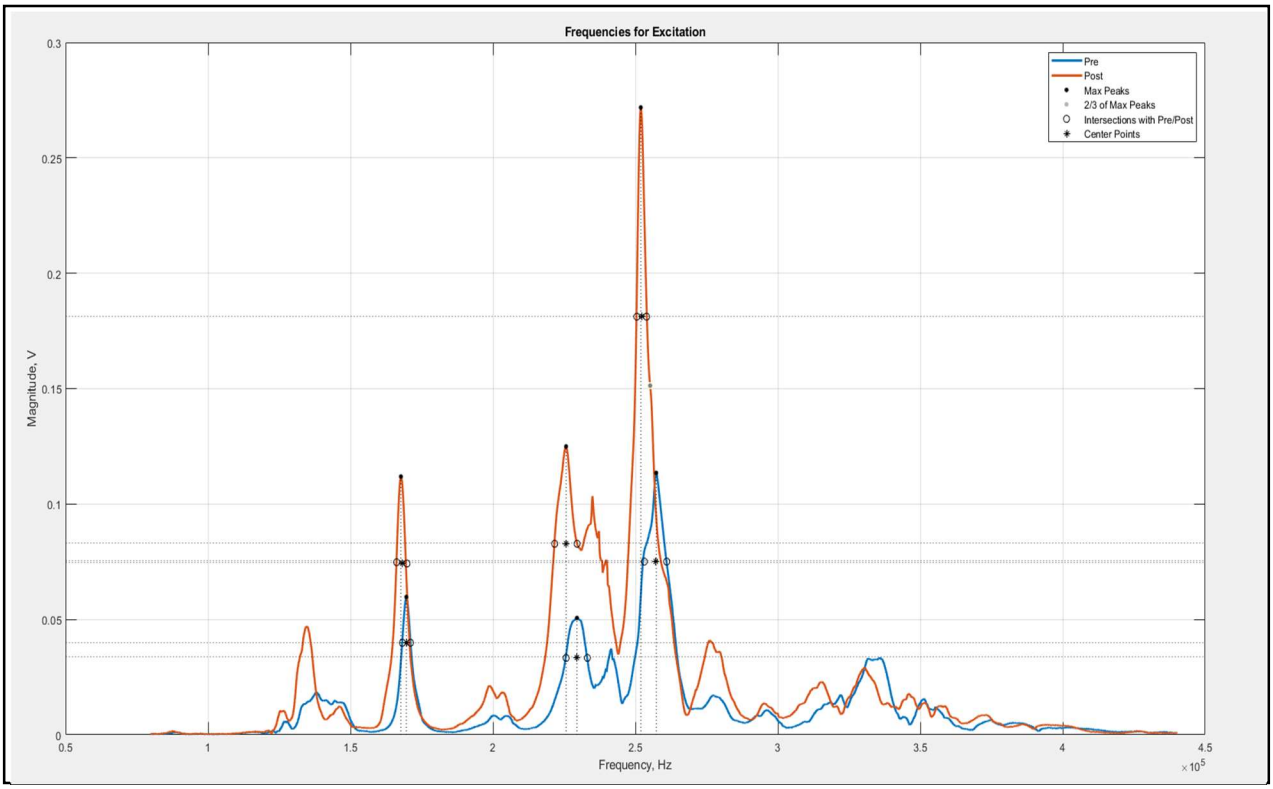

FIGURE 14: STEP 3 OF MATLAB PROTOCOL: MIDPOINT OUTPUT

3.7 STATISTICAL ANALYSIS

All significance calculations were done using Design-Expert. Design-Expert is a software package designed to help with the entire DOE process and analysis. The study was set up as a triple factor, triple response design with varying numbers of replicates. Factor A was 'Bone Position' (femur or humerus), Factor B was 'Species', and Factor C was 'Bone Composition' (compact bone or spongy bone). Response 1, the main response, was 'Shift'. These values were those values generated by the aforementioned MATLAB code. Because individual modes shifting in either direction could be a potential point of interest, there was a second response created: Response 2 – 'Absolute Individual Shift'. This response was calculated by taking the

absolute value of the shifts experienced by the three peaks of interest and averaging those values together. For the warm-blooded species, these two responses were almost always identical (almost every shift was right -> left). However, the individual peak shifts for the cold-blooded samples alternated between negative and positive shifts, so the difference between Response 1 and Response 2 was often significant. Response 3 was generated as a result of a noticed trend. The magnitude is often neglected in excitation frequency plots. The frequency is assumed to be one of the sample's modes if the magnitude of the response is significant. The actual value of that magnitude matters not. That having been said, it was observed that the area under the curve (AUC) changed substantially more for the endotherms, so AUC was calculated and added as Response 3. The table showing all factors, responses, and values can be seen below:

TABLE 4: DESIGN-EXPERT INPUT TABLE SHOWING FEATURES AND RESPONSES

Std	Run	Factor 1 A:BonePosition	Factor 2 B:Species	Factor 3 C:BoneComposi...	Response 1 Shift	Response 2 Abs Individual S...	Response 3 Delta AUC
1	1	Femur	Cow	Compact	-3427	3427	3540
13	2	Femur	Cow	Compact	-5959	5959	1450
14	3	Femur	Cow	Compact	-2617	2617	1060
15	4	Femur	Cow	Compact	-1881	1881	4480
16	5	Femur	Cow	Compact	-2646	2646	1680
17	6	Femur	Cow	Compact	-1411	1411	2190
2	7	Humerus	Cow	Compact	-1117	1528	2230
12	8	Humerus	Cow	Compact	-1323	1323	1210
3	9	Femur	Alligator	Compact	-265	340	-349
18	10	Femur	Alligator	Compact	-59	1764	325
19	11	Femur	Alligator	Compact	0	176.333	1480
20	12	Femur	Alligator	Compact	120.666	709.3	1160
7	13	Femur	Alligator	Spongey	-50	369	-959
21	14	Femur	Alligator	Spongey	-353	646	300
8	15	Humerus	Alligator	Spongey	-67	874	-920
27	16	Humerus	Alligator	Spongey	-370	839.666	
28	17	Humerus	Alligator	Spongey	0	671.666	190
29	18	Humerus	Alligator	Spongey	-403	470.333	341
4	19	Humerus	Alligator	Compact	-75	378	1040
22	20	Humerus	Alligator	Compact	-1399	1398.5	720
23	21	Humerus	Alligator	Compact	-1172	1247.5	-750
24	22	Humerus	Alligator	Compact	-101	134.666	-1430
25	23	Humerus	Alligator	Compact	617	617	452
26	24	Humerus	Alligator	Compact	29	147.333	2190
6	25	Humerus	Horse	Compact	-2999	2999	2300
9	26	Humerus	Horse	Compact	-2318	2318	5560
5	27	Femur	Horse	Compact	-1713	1713	-307
10	28	Femur	Horse	Compact	-1705	1705	2170
11	29	Femur	Horse	Compact	-2969	2969	-717

The statistical analysis was then approached and completed in its entirety for one response followed by another. Response 1 – 'Shift' was analyzed first. A Half-Normal plot was generated as the first step toward determining the significance of the factors. This plot suggested that Factor B – 'Species' had a significant impact on Response 1. That plot can be seen below:

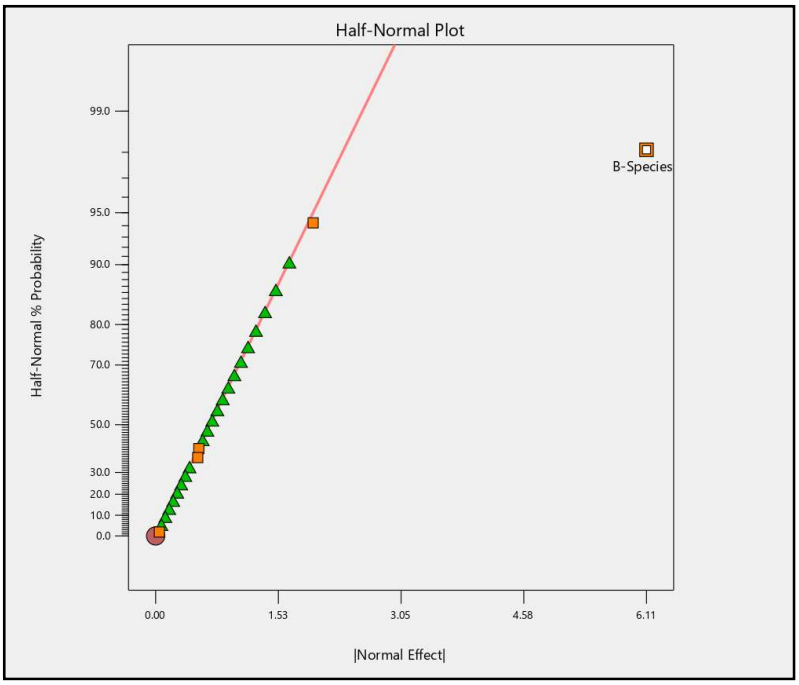

FIGURE 15: HALF-NORMAL PLOT FOR RESPONSE 1: 'SHIFT'

Next, an analysis of variance was computed (ANOVA). The Model F-value of 20.72 implied the model was significant. There was only a 0.01% chance that an F-value this large could occur due to noise. P values less than 0.05 generally indicate that a model term is significant. The p-value was found to be less than 0.0001, thus the model term was highly significant. The lack of fit f-value was 1.26, which implied that the lack of fit was not significant relative to the pure error (this is a good thing).

TABLE 5: ANOVA FOR FACTOR B'S EFFECT ON RESPONSE 1

Source	Sum of Squares	df	Mean Square	F-value	p-value	
Model	3.632E+07	2	1.816E+07	20.72	< 0.0001	significant
B-Species	3.632E+07	2	1.816E+07	20.72	< 0.0001	
Residual	2.280E+07	26	8.768E+05			
Lack of Fit	5.254E+06	5	1.051E+06	1.26	0.3185	not significant
Pure Error	1.754E+07	21	8.353E+05			
Cor Total	5.912E+07	28				

The significance of 'Species' as a factor in a sample's excitation frequency shift as a result of thermal cycling can be visualized by having the Shift on the y-axis and the three species on the x-axis. That plot with error bars can be seen below:

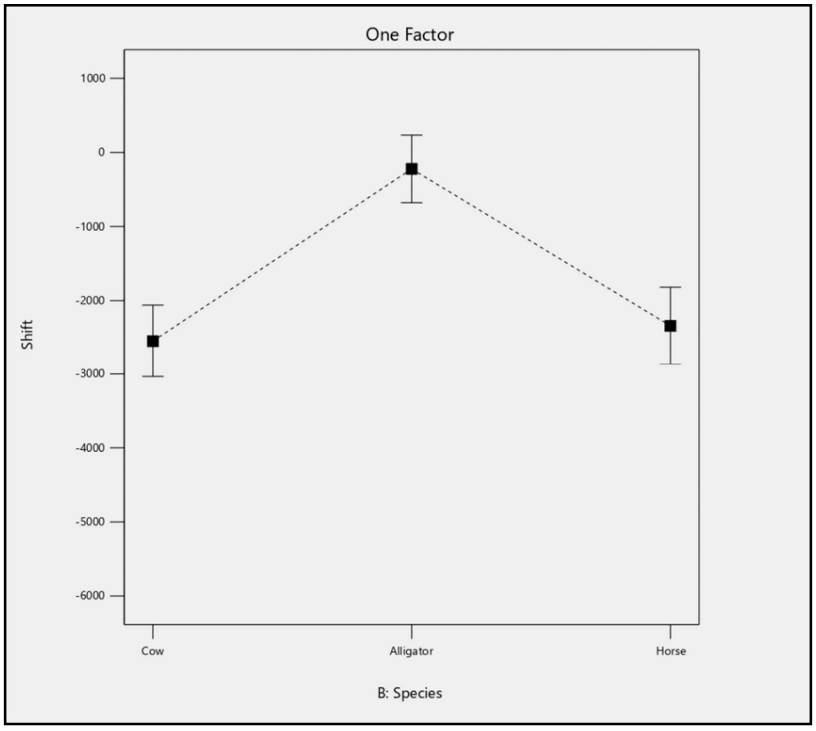

FIGURE 16: ONE FACTOR PLOT FOR RESPONSE 1: 'SHIFT'

Response 2 – ‘Absolute Individual Shift’ was then analyzed. A Half-Normal plot was generated as the first step toward determining the significance of the factors. This plot suggested that Factor B – ‘Species’ had a significant impact on Response 2. That plot can be seen below:

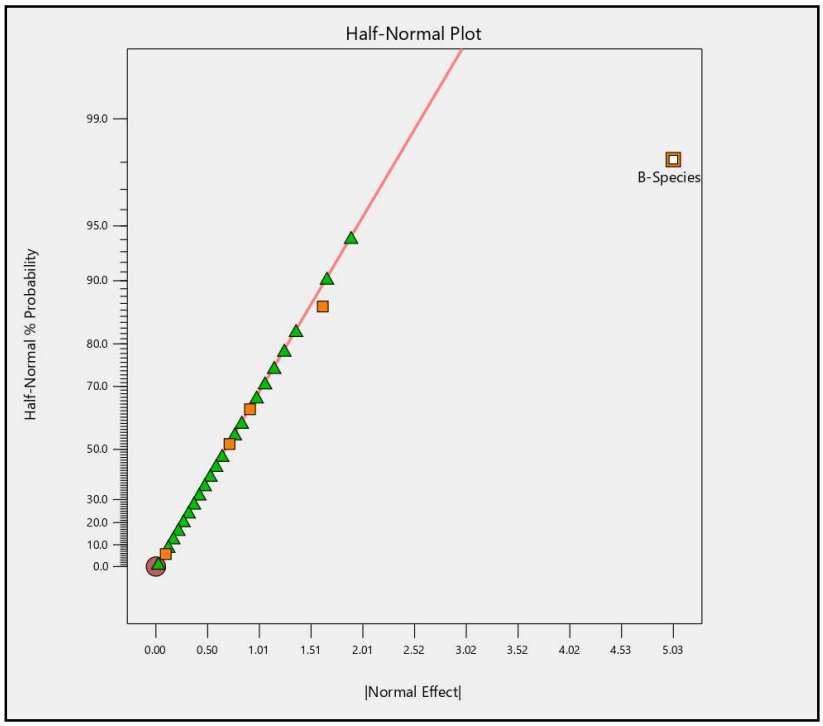

FIGURE 17: HALF-NORMAL PLOT FOR RESPONSE 2: ‘ABSOLUTE INDIVIDUAL SHIFT’

Next, an analysis of variance was computed (ANOVA). The Model F-value of 14.53 implied the model was significant. There was only a 0.01% chance that an F-value this large could occur due to noise. P values less than 0.05 generally indicate that a model term is significant. The p-value was found to be less than 0.0001, thus the model term was highly significant. The lack of fit f-value was 0.98, which implies that the lack of fit was not significant relative to the pure error (again, this is a good thing).

TABLE 6: ANOVA FOR FACTOR B'S EFFECT ON RESPONSE 2

Source	Sum of Squares	df	Mean Square	F-value	p-value	
Model	2.411E+07	2	1.206E+07	14.53	< 0.0001	significant
B-Species	2.411E+07	2	1.206E+07	14.53	< 0.0001	
Residual	2.157E+07	26	8.296E+05			
Lack of Fit	4.095E+06	5	8.189E+05	0.9840	0.4507	not significant
Pure Error	1.748E+07	21	8.322E+05			
Cor Total	4.568E+07	28				

The significance of 'Species' as a factor in Response 2 can be visualized by the plot below:

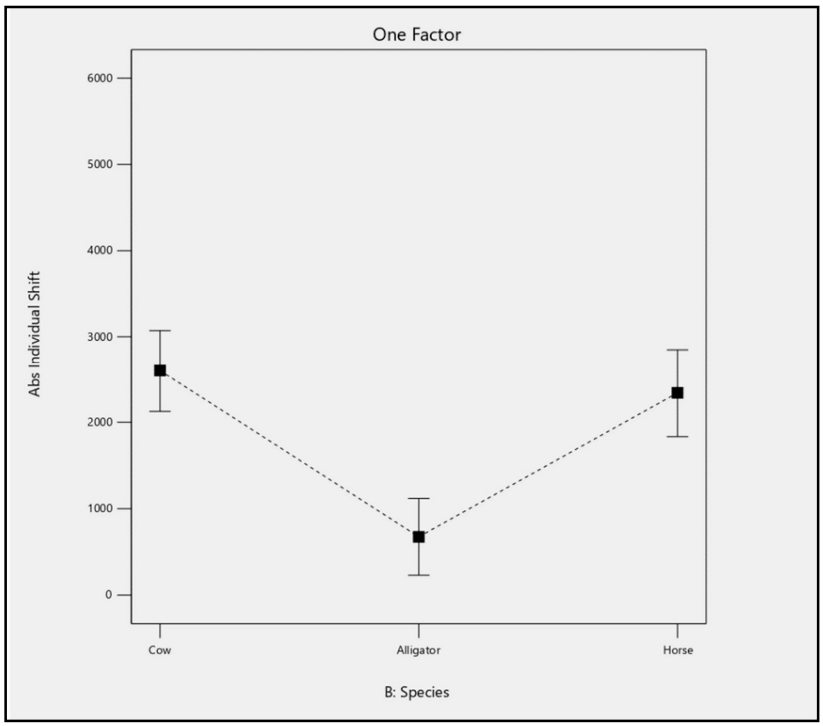

FIGURE 18: ONE FACTOR PLOT FOR RESPONSE 2

Finally, Response 3 – 'AUC' was analyzed. A Half-Normal plot was generated as the first step toward determining the significance of the factors. This plot suggested that Factor B – 'Species' had a significant impact on Response 3. That plot can be seen below:

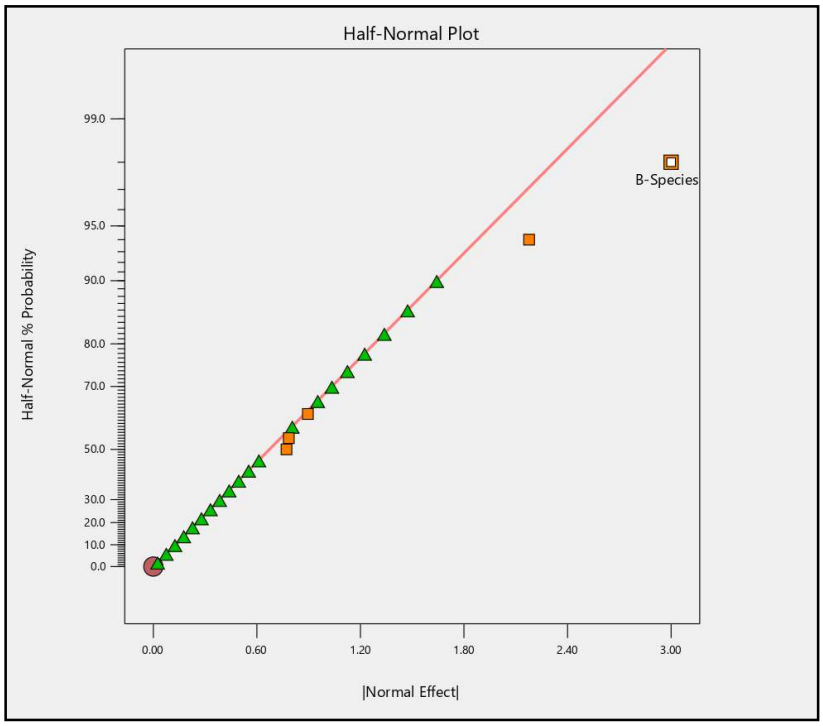

FIGURE 19: HALF-NORMAL PLOT FOR RESPONSE 3

Next, an analysis of variance was computed (ANOVA). The Model F-value of 5.93 implied the model was significant. There was only a 0.78% chance that an F-value this large could occur due to noise. P values less than 0.05 generally indicate that a model term is significant. The p-value was found to be less than 0.0078, thus the model term was highly significant. The lack of fit f-value was 2.22, which implies that the lack of fit was not significant relative to the pure error.

TABLE 7: ANOVA FOR FACTOR B'S EFFECT ON RESPONSE 3

Source	Sum of Squares	df	Mean Square	F-value	p-value	
Model	2.344E+07	2	1.172E+07	5.93	0.0078	significant
B-Species	2.344E+07	2	1.172E+07	5.93	0.0078	
Residual	4.942E+07	25	1.977E+06			
Lack of Fit	1.764E+07	5	3.529E+06	2.22	0.0923	not significant
Pure Error	3.178E+07	20	1.589E+06			
Cor Total	7.286E+07	27				

The significance of 'Species' as a factor in Response 3 can be visualized by the plot below:

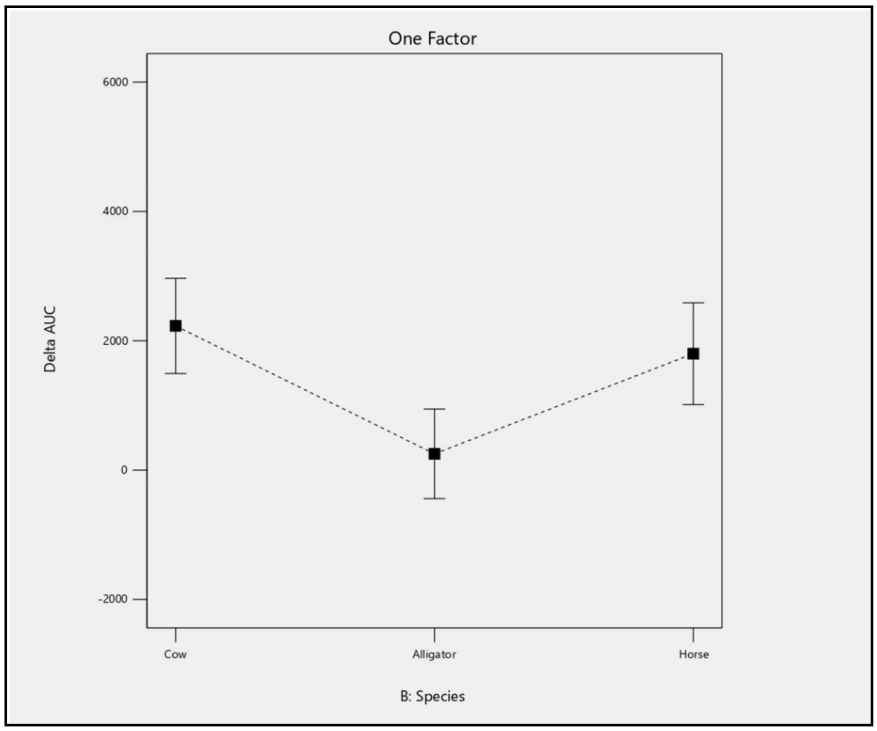

FIGURE 20: ONE FACTOR PLOT FOR RESPONSE 3

CHAPTER 4: CONCLUSIONS

This work investigated the hypothesis: “Have cold-blooded animals developed a resistance to thermal cycling?”. To answer this question, bone samples were harvested from both cold-blooded and warm-blooded species. Those samples were processed, weighed, imaged, and measured before undergoing the first series of resonant ultrasound spectroscopy analyses. That initial RUS protocol created a baseline plot of resonant frequencies. Those frequencies can be used to calculate or back-calculate a multitude of physical properties (elastic moduli, Poisson’s ratio, ductility, etc.), but more importantly, that plot of resonant frequencies acts as a fingerprint that tells the story of any given sample’s elastic makeup.

Following the first round of RUS analyses, all 29 samples were subjugated to a month of thermal cycling at natural temperatures but with accelerated ramp times. The samples were removed from the thermal chamber and again weighed, imaged, and measured before undergoing the second and final round of RUS analyses.

A MATLAB code was written to quantify any shifts that may or may not have arisen as a result of the thermal cycling. Those shifts in resonant / excitation frequencies were then averaged together to create a single quantifier for the shifts experienced by each of the 29 samples.

Those quantifiers were then characterized via Design-Expert. This statistical analysis proved with high certainty what the plots had already suggested: **Alligator, a cold-blooded species, was minimally affected by thermal cycling, whereas both cow and horse samples,**

warm-blooded species, were both dramatically altered in their elastic profile as a direct result of thermal cycling.

4.1 NOTE ON EXPERIMENTAL FINDINGS

It is important to discuss what this data does not prove. The data to support the stark difference between the two sample types (cold-blooded and warm-blooded) was indeed exceptionally significant. That having been said, it cannot definitively be said that cold-blooded animals have a heightened resilience to the negative effects of thermal cycling. Saying as much would suggest that a much larger sample size (more species from both ectotherm and endotherm classes) had been characterized.

4.2 FUTURE DIRECTIONS AND ADJUSTMENTS

For warm-blooded samples, the magnitude of the response to thermal cycling far surpassed all expectations. It was of course hypothesized that the elastic makeup of warm-blooded samples would distort more so than the cold-blooded samples, but for the warm-blooded frequencies to have shifted more than 11x that of the cold-blooded frequencies is both remarkable and highly validating.

The findings presented in this paper have undoubtedly unlocked a door into an entirely new regime of research. If cold-blooded species really do have this significant of a resistance to thermal cycling, the implications and applications are vast, to say the least. All of this having been said, it is believed that one or more controls would need to be implemented in order to confidently deny or accept the hypothesis. One factor with a known impact on the composition and strength of bone is diet. In this study, the cold-blooded samples were harvested from

carnivores and the warm-blooded samples were harvested from herbivores. The lack of this control was less of a design flaw and more of a resource drought. To prepare samples large enough for RUS analysis, the bones from which the samples are cored must be relatively large in diameter. There were extremely few cold-blooded species that satisfied the size requisite, and no species that satisfied both the size and diet requisites (large, cold-blooded herbivore). In future studies, it would be prudent to prepare samples from a large, carnivorous, warm-blooded species (wild cats, bears, wolves, etc.). In doing so, the design would be capable of either proving or disproving diet's role in a bone's ability to withstand the effects of thermal cycling. Additionally, it is believed that the implementation of a fluidic thermal cycling apparatus would more accurately model physiologic conditions.

List of References

References

1. Rohrig, B. Chilling Out, Warming Up. *ChemMatters* (2013).
2. Boskey, A. L. Bone composition: relationship to bone fragility and antiosteoporotic drug effects. (2013) doi:10.1038/bonekey.2013.181.
3. Kö Hler, M. & Moyà -Solà, S. *Physiological and life history strategies of a fossil large mammal in a resource-limited environment*. www.pnas.orgcgidoi10.1073pnas.0813385106.
4. Visscher, W. M., Migliori, A., Bell, T. M. & Reinerr, R. A. *On the normal modes of free vibration of inhomogeneous and anisotropic elastic objects ß*.
5. Holland, R. *Resonant Properties of Piezoelectric Ceramic Rectangular Parallelepipeds*. http://acousticalsociety.org/content/terms.
6. Migliori, A. *et al.* Resonant ultrasound spectroscopic techniques for measurement of the elastic moduli of solids. *Physica B: Condensed Matter* **183**, 1–24 (1993).
7. Muller, M. *et al.* Nonlinear resonant ultrasound spectroscopy (NRUS) applied to damage assessment in bone. *J Acoust Soc Am* **118**, 3946–3952 (2005).
8. Li, G. & Gladden, J. R. High Temperature Resonant Ultrasound Spectroscopy: A Review. *International Journal of Spectroscopy* **2010**, 1–13 (2010).
9. Cai, X. *et al.* Anisotropic elastic properties of human cortical bone tissue inferred from inverse homogenization and resonant ultrasound spectroscopy. *Materialia (Oxf)* **11**, (2020).
10. Daoui, H., Cai, X., Boubenider, F., Laugier, P. & Grimal, Q. Assessment of trabecular bone tissue elasticity with resonant ultrasound spectroscopy. *Journal of the Mechanical Behavior of Biomedical Materials* **74**, 106–110 (2017).
11. Lee, T., Lakes, R. S. & Lal, A. Investigation of bovine bone by resonant ultrasound spectroscopy and transmission ultrasound. *Biomechanics and Modeling in Mechanobiology* **1**, 165–175 (2002).
12. Semaan, M. *et al.* Assessment of elastic coefficients of child cortical bone using resonant ultrasound spectroscopy. doi:10.1016/j.jmbbm.2018.09.044ï.
13. Cai, X., Peralta, L. & Gouttenoire, P.-J. Quantification of stiffness measurement errors in resonant ultrasound spectroscopy of human cortical bone. *Citation: The Journal of the Acoustical Society of America* **142**, 2755 (2017).
14. Zapata, U. *et al.* Material properties of mandibular cortical bone in the American alligator, Alligator mississippiensis. *Bone* **46**, 860–867 (2010).

15. Kim, B. & Yang, H. Temperature sensor assisted lifetime enhancement of satellite embedded systems via multi-core task mapping and DVFS. *Sensors (Switzerland)* **19**, (2019).

16. Bao, S. *et al.* Effect of thermal cycling on mechanical and microstructural properties of heat-treated Ti-6Al-4V alloy You may also like Effects of heat treatment on martensitic transformation and wear resistance of as-cast 60NiTi alloy The Palomar Transient Factory Core-collapse Supernova Host-galaxy Sample. I. Host-galaxy Distribution Functions and Environment Dependence of Core-collapse Supernovae Effect of thermal cycling on mechanical and microstructural properties of heat-treated Ti-6Al-4V alloy. (2022) doi:10.1088/2053-1591/ac487d.

17. Agbadua, S. A., Ogonna Mgbemena, C., Mgbemena, C. E. & Chima, L. O. *Thermal Cycling Effects on the Fatigue Behaviour of Low Carbon Steel*. *Journal of Minerals & Materials Characterization & Engineering* vol. 10 (2011).

18. Miyazaki, M., Sato, M., Onose, H. & Moore, B. K. Influence of thermal cycling on dentin bond strength of two-step bonding systems. *Am J Dent* **11**, 118—122 (1998).

19. Nikaido, T. *et al. Evaluation of thermal cycling and mechanical loading on bond strength of a self-etching primer system to dentin*. www.elsevier.com/locate/dental.

20. RapidTherm Inc. *RapidTherm® Operators Manual With the IDEC Touchscreen Controller Revision 16.40*.

21. Kinney, J. H. *et al.* Resonant ultrasound spectroscopy measurements of the elastic constants of human dentin. *Journal of Biomechanics* **37**, 437–441 (2004).

22. Jordan Hawes. Thermal Regulation Graph. (2018).

23. RUS ACQUISITION AND PLOT.

24. Farhad Farzbod, O. E. S.-E. Resonant Ultrasound Spectroscopy: Sensitivity Analysis for Isotropic Materials and Anisotropic Materials With Cubic Symmetry. *Journal of Vibration and Acoustics* **141**, (2019).

25. RAPIDTHERM THERMAL CHAMBER.

26. Resonant ultrasound spectroscopy - Wikipedia

Appendix

APPENDIX A:

```
%-------------------------------------------------------------------------%
%--------------Clear the command window and all variables-----------------%
%-------------------------------------------------------------------------%
clc
clear
%-------------------------------------------------------------------------%
%-------------------------Load & separate the data-----------------------%
%-------------------------------------------------------------------------%
importfile1 = readtable('CF1_A_Pre.txt');
importfile2 = readtable('CF1_A_Post.txt');
pre_1 = table2array(importfile1(:,1));
pre_2 = table2array(importfile1(:,2));
post_1 = table2array(importfile2(:,1));
post_2 = table2array(importfile2(:,2));
%-------------------------------------------------------------------------%
%-----------------------------Find Peaks----------------------------------%
%-------------------------------------------------------------------------%
[pks_pre, locs_pre]= findpeaks(pre_2, pre_1, 'MinPeakDistance', 10000,
'MinPeakHeight', 0.025, 'SortStr','descend');
[pks_post, locs_post ]= findpeaks(post_2, post_1, 'MinPeakDistance', 10000,
'MinPeakHeight', 0.025, 'SortStr','descend');
%-------------------------------------------------------------------------%
%---------------------------------Plots-----------------------------------%
%-------------------------------------------------------------------------%
%Plot #1 find peaks
figure(1);
plot(pre_1, pre_2, 'linewidth', 2);
hold on
plot(post_1, post_2, 'linewidth', 2);
hold on
findpeaks(pre_2, pre_1, 'MinPeakDistance', 10000, 'MinPeakHeight', 0.025)
text(locs_pre+.02,pks_pre,num2str((1:numel(pks_pre))'))
hold on
findpeaks(post_2, post_1, 'MinPeakDistance', 10000, 'MinPeakHeight', 0.025)
text(locs_post+.02,pks_post,num2str((1:numel(pks_post))'))
title({['Frequencies for Excitation']});
legend('Pre', 'Post');
xlabel('Frequency, Hz')
ylabel('Magnitude, V')
grid on
%Pick the three peaks of interest
pre_x1 = locs_pre(2);
pre_y1 = pks_pre(2);
post_x1 = locs_post(3);
post_y1 = pks_post(3);
```

```
pre_x2 = locs_pre(3);
pre_y2 = pks_pre(3);
post_x2 = locs_post(2);
post_y2 = pks_post(2);
pre_x3 = locs_pre(1);
pre_y3 = pks_pre(1);
post_x3 = locs_post(1);
post_y3 = pks_post(1);
%Multiply y values by 2/3
pre_y1_23 = pre_y1*2/3;
post_y1_23 = post_y1*2/3;
pre_y2_23 = pre_y2*2/3;
post_y2_23 = post_y2*2/3;
pre_y3_23 = pre_y3*2/3;
post_y3_23 = post_y3*2/3;
%Get intersections
[x_y1_23_pre y_y1_23_pre] = intersections(pre_1, pre_2, [200 400000], [pre_y1_23
pre_y1_23]);
[x_y2_23_pre y_y2_23_pre] = intersections(pre_1, pre_2, [200 400000], [pre_y2_23
pre_y2_23]);
[x_y3_23_pre y_y3_23_pre] = intersections(pre_1, pre_2, [200 400000], [pre_y3_23
pre_y3_23]);
[x_y1_23_post y_y1_23_post] = intersections(post_1, post_2, [200 400000], [post_y1_23
post_y1_23]);
[x_y2_23_post y_y2_23_post] = intersections(post_1, post_2, [200 400000], [post_y2_23
post_y2_23]);
[x_y3_23_post y_y3_23_post] = intersections(post_1, post_2, [200 400000], [post_y3_23
post_y3_23]);
grayColor = [0.7 0.7 0.7];
%l1, l2...l6 for legend purposes
%Plot the peaks of interest
figure(2);
l1 = plot(pre_1, pre_2, 'linewidth', 2);
hold on
l2 = plot(post_1, post_2, 'linewidth', 2);
hold on
l3 = plot(pre_x1, pre_y1, '.k', 'MarkerSize', 12);
hold on
plot(pre_x2, pre_y2, '.k', pre_x3, pre_y3, '.k', 'MarkerSize', 12);
hold on
plot(post_x1, post_y1, '.k', post_x2, post_y2, '.k', post_x3, post_y3, '.k',
'MarkerSize', 12);
hold on
l4 = plot(pre_x1, pre_y1_23, '.', 'Color', grayColor, 'MarkerSize', 12);
hold on
plot(pre_x2, pre_y2_23, '.', pre_x3, pre_y3_23, '.', 'Color', grayColor,
'MarkerSize', 12);
hold on
plot(post_x1, post_y1_23, '.', post_x2, post_y2_23, '.', post_x3, post_y3_23, '.',
'Color', grayColor,'MarkerSize', 12);
hold on
plot([pre_x1 pre_x1],[0 pre_y1], ':k', [pre_x2 pre_x2],[0 pre_y2], ':k', [pre_x3
pre_x3],[0 pre_y3], ':k')
hold on
```

```
plot([post_x1 post_x1],[0 post_y1], ':k', [post_x2 post_x2],[0 post_y2], ':k',
[post_x3 post_x3],[0 post_y3], ':k')
hold on
z=yline(pre_y1_23, ':k');
hold on
yline(pre_y2_23, ':k');
hold on
yline(pre_y3_23, ':k');
hold on
yline(post_y1_23, ':k');
hold on
yline(post_y2_23, ':k');
hold on
yline(post_y3_23, ':k');
hold on
l5 = plot(x_y1_23_pre, y_y1_23_pre, 'ob');
hold on
plot(x_y2_23_pre, y_y2_23_pre, 'ob', x_y3_23_pre, y_y3_23_pre, 'ob');
hold on
l6 = plot(x_y1_23_post, y_y1_23_post, 'or');
hold on
plot(x_y2_23_post, y_y2_23_post, 'or', x_y3_23_post, y_y3_23_post, 'or');
title({['Frequencies for Excitation']});
legend([l1 l2 l3 l4 l5 l6], 'Pre', 'Post', 'Max Peaks', '2/3 of Max Peaks',
'Intersections wiht Pre', 'Intersections with Post');
xlabel('Frequency, Hz')
ylabel('Magnitude, V')
grid on
[xi, yi] = ginput;
%Center points
centerx(1) = (xi(1)+xi(2))/2;
centery(1) = (yi(1)+yi(2))/2;
centerx(2) = (xi(3)+xi(4))/2;
centery(2) = (yi(3)+yi(4))/2;
centerx(3) = (xi(5)+xi(6))/2;
centery(3) = (yi(5)+yi(6))/2;
centerx(4) = (xi(7)+xi(8))/2;
centery(4) = (yi(7)+yi(8))/2;
centerx(5) = (xi(9)+xi(10))/2;
centery(5) = (yi(9)+yi(10))/2;
centerx(6) = (xi(11)+xi(12))/2;
centery(6) = (yi(11)+yi(12))/2;
%Plot the final graph with the center points
figure(3);
l1 = plot(pre_1, pre_2, 'linewidth', 2);
hold on
l2 = plot(post_1, post_2, 'linewidth', 2);
hold on
l3 = plot(pre_x1, pre_y1, '.k', 'MarkerSize', 12);
hold on
plot(pre_x2, pre_y2, '.k', pre_x3, pre_y3, '.k', 'MarkerSize', 12);
hold on
plot(post_x1, post_y1, '.k', post_x2, post_y2, '.k', post_x3, post_y3, '.k',
'MarkerSize', 12);
hold on
```

```
l4 = plot(pre_x1, pre_y1_23, '.', 'Color', grayColor, 'MarkerSize', 12);
hold on
plot(pre_x2, pre_y2_23, '.', pre_x3, pre_y3_23, '.', 'Color', grayColor,
'MarkerSize', 12);
hold on
plot(post_x1, post_y1_23, '.', post_x2, post_y2_23, '.', post_x3, post_y3_23, '.',
'Color', grayColor,'MarkerSize', 12);
hold on
plot([pre_x1 pre_x1],[0 pre_y1], ':k', [pre_x2 pre_x2],[0 pre_y2], ':k', [pre_x3
pre_x3],[0 pre_y3], ':k')
hold on
plot([post_x1 post_x1],[0 post_y1], ':k', [post_x2 post_x2],[0 post_y2], ':k',
[post_x3 post_x3],[0 post_y3], ':k')
hold on
z=yline(pre_y1_23, ':k');
hold on
yline(pre_y2_23, ':k');
hold on
yline(pre_y3_23, ':k');
hold on
yline(post_y1_23, ':k');
hold on
yline(post_y2_23, ':k');
hold on
yline(post_y3_23, ':k');
hold on
l5 = plot(xi, yi, 'ok');
hold on
l6 = plot(centerx, centery, '*k');
title({['Frequencies for Excitation']});
legend([l1 l2 l3 l4 l5 l6], 'Pre', 'Post', 'Max Peaks', '2/3 of Max Peaks',
'Intersections with Pre/Post', 'Center Points');
xlabel('Frequency, Hz')
ylabel('Magnitude, V')
grid on
%Print out center points
fprintf('Center point 1:\n');
fprintf('Post = %6.3f Pre = %6.3f\n', centerx(1), centerx(2));
fprintf('Center point 2:\n');
fprintf('Post = %6.3f Pre = %6.3f\n', centerx(3), centerx(4));
fprintf('Center point 3:\n');
fprintf('Post = %6.3f Pre = %6.3f\n', centerx(5), centerx(6));
```

HORSE HUMERUS A

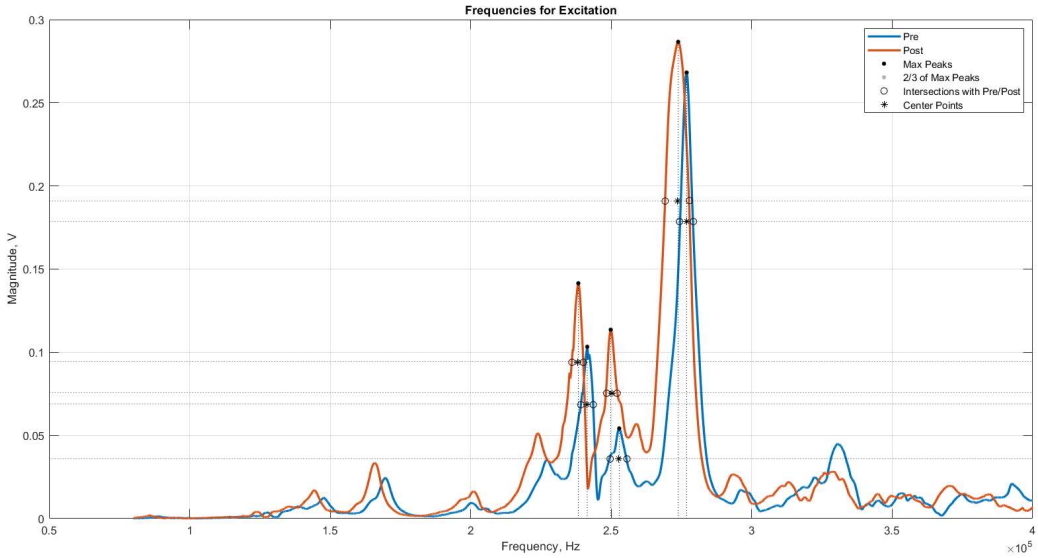

HORSE HUMERUS B

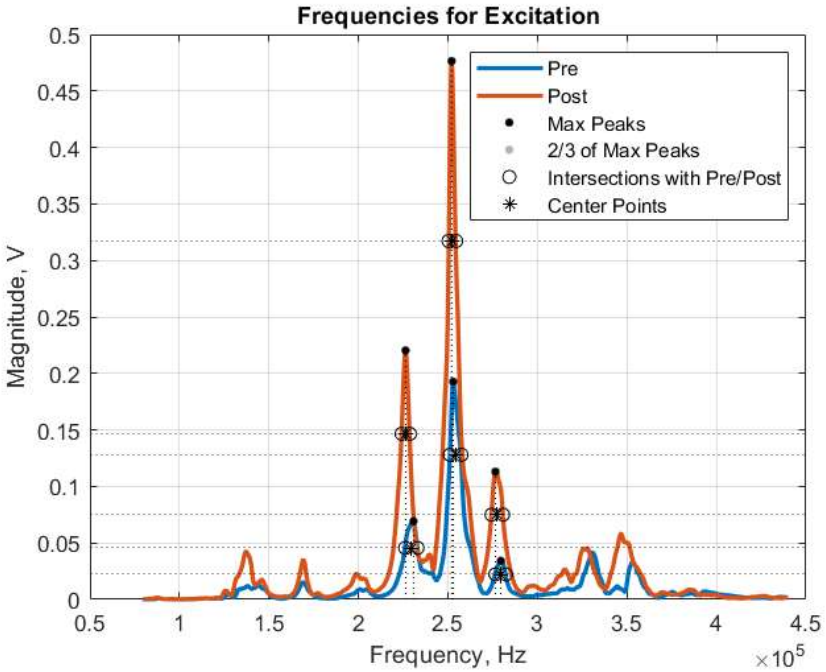

HORSE FEMUR 1A

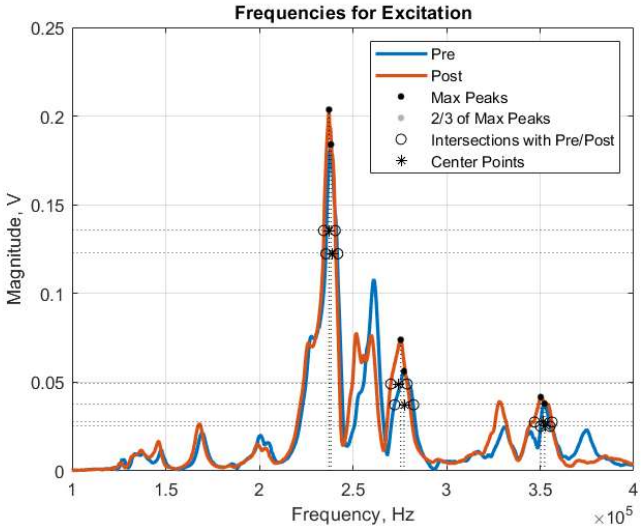

HORSE FEMUR 1B

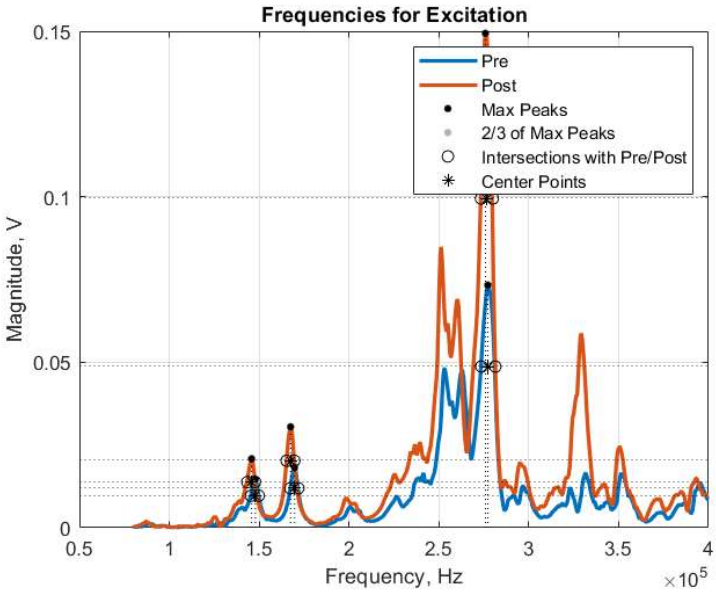

HORSE FEMUR 1C

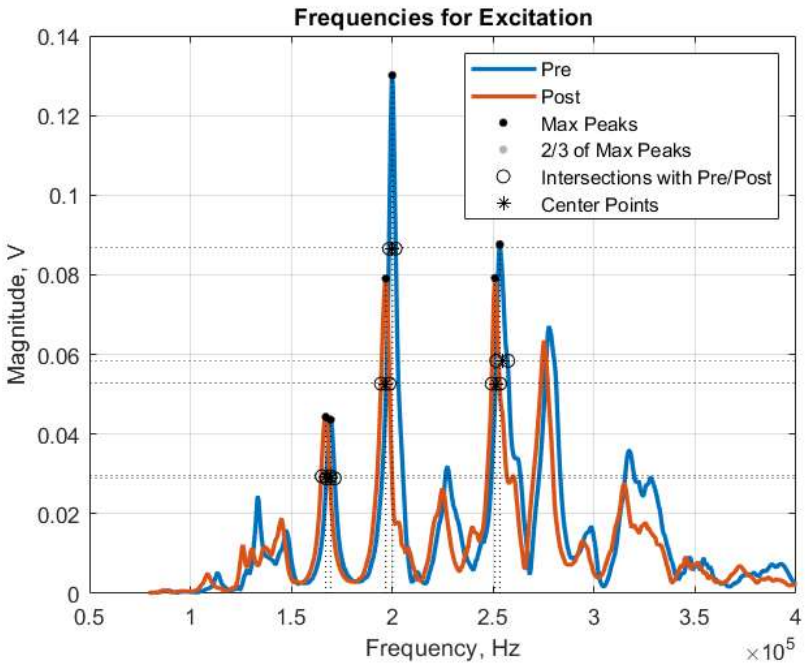

COW HUMERUS 1A

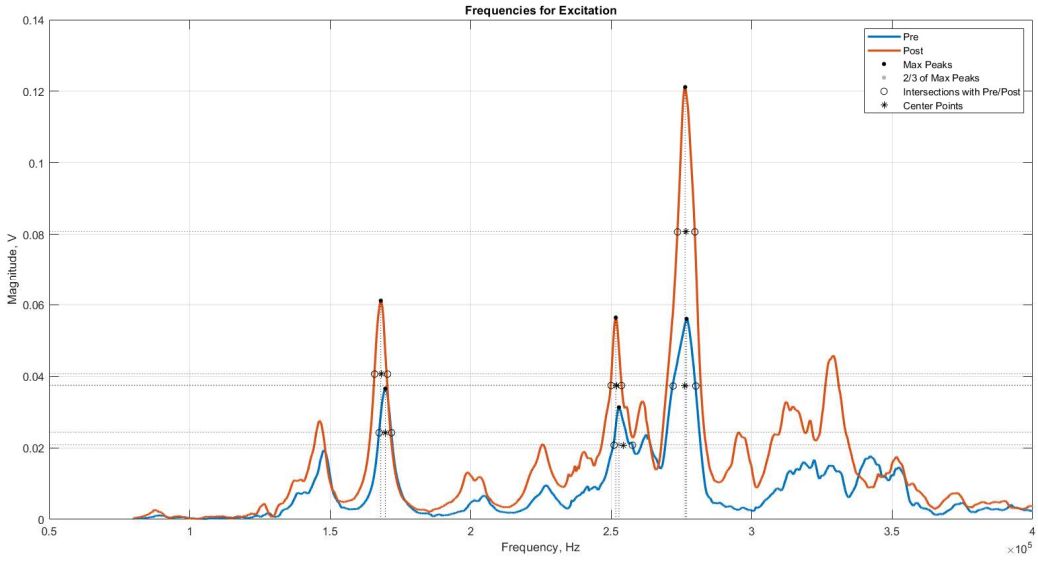

COW HUMERUS 1B

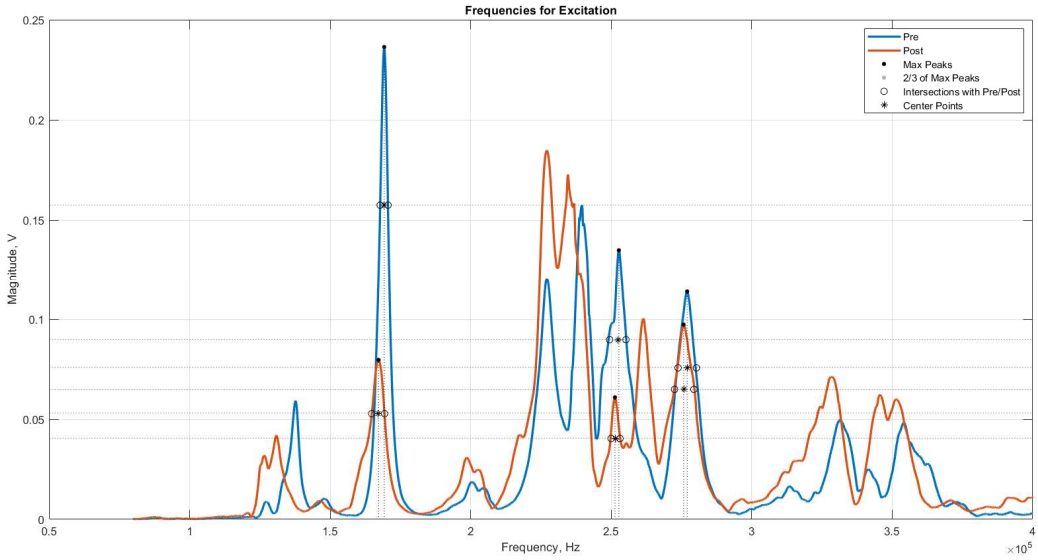

COW FEMUR 1A

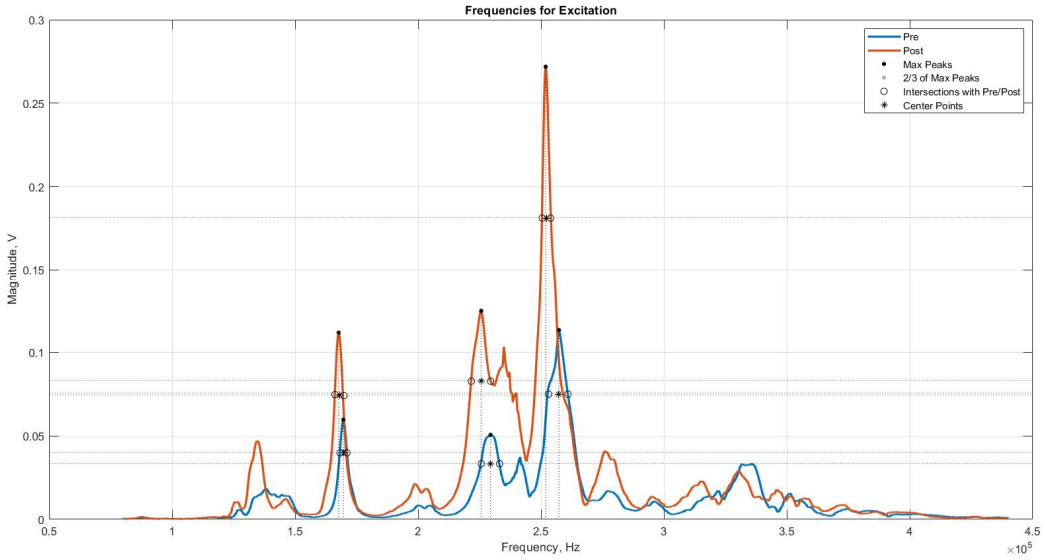

COW FEMUR 2A

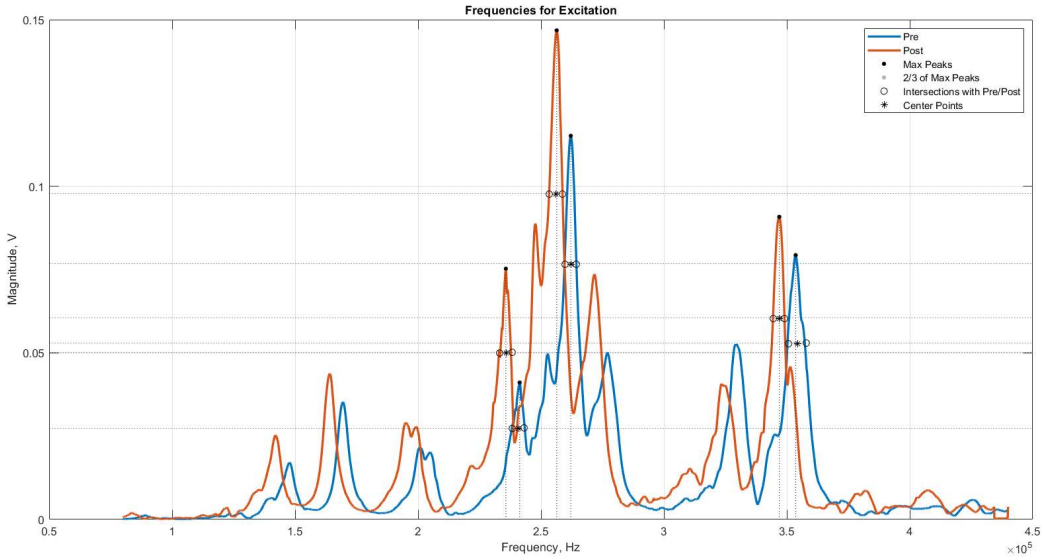

COW FEMUR 2B

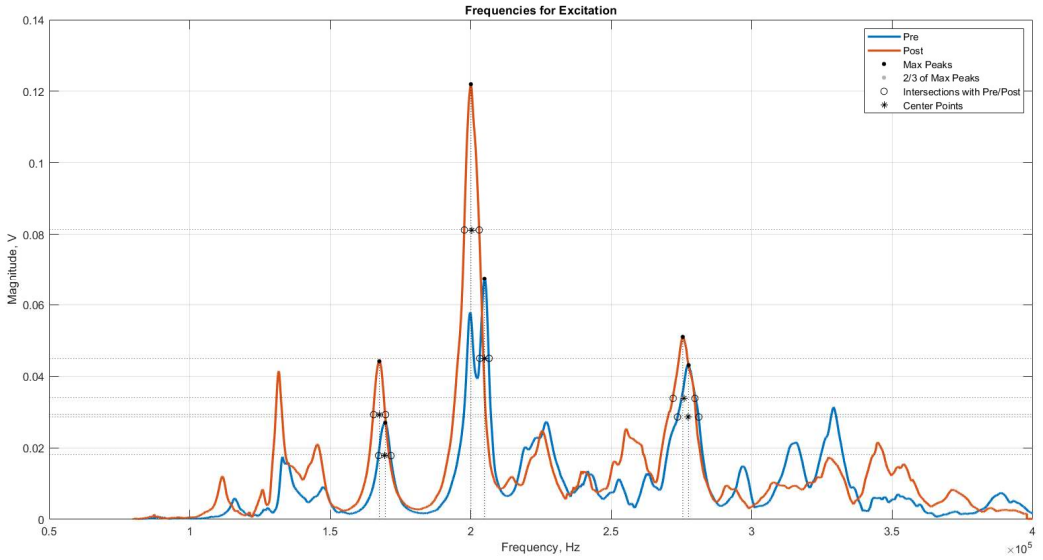

COW FEMUR 3A

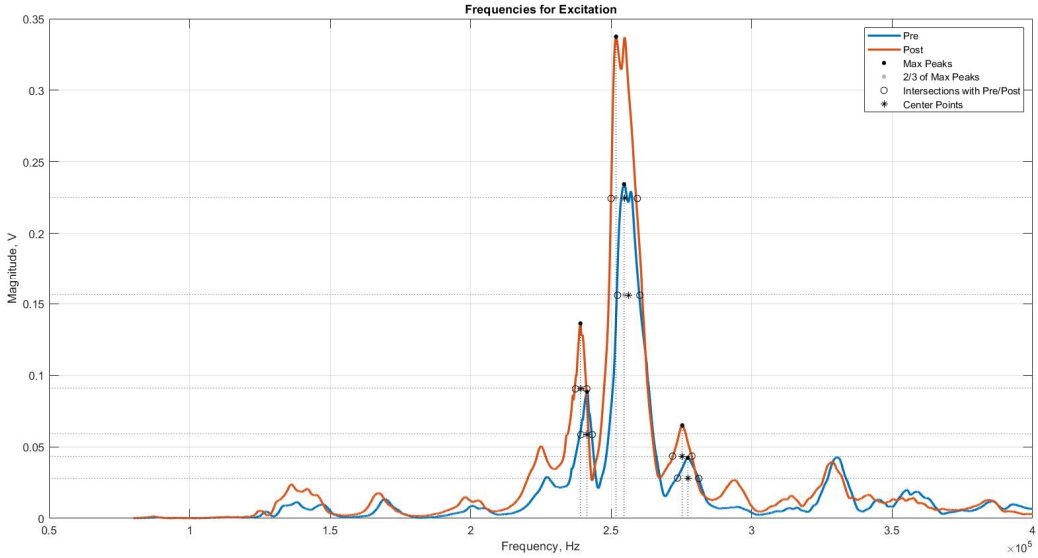

COW FEMUR 3B

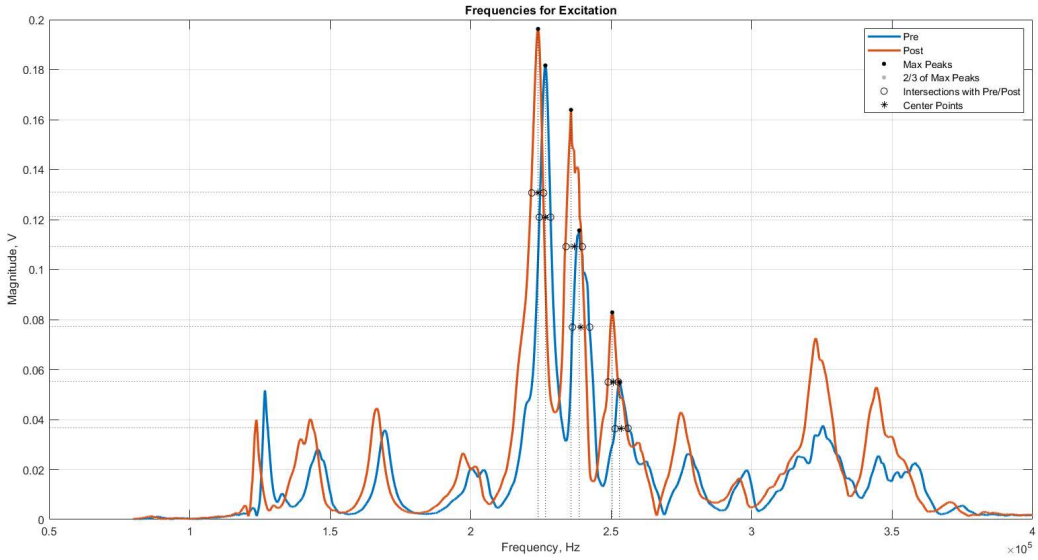

COW FEMUR 3C

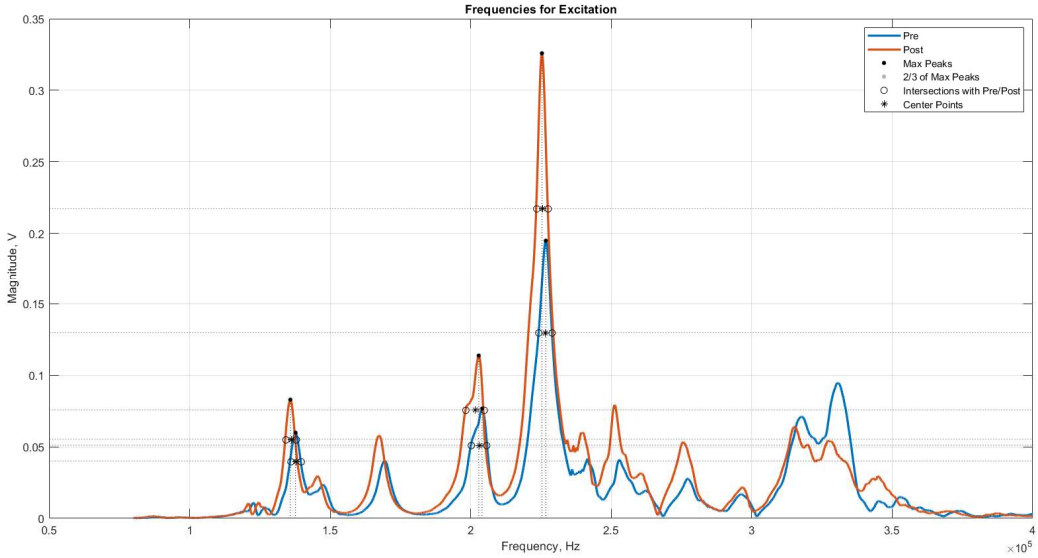

ALLIGATOR FEMUR 1 SPONGY 1

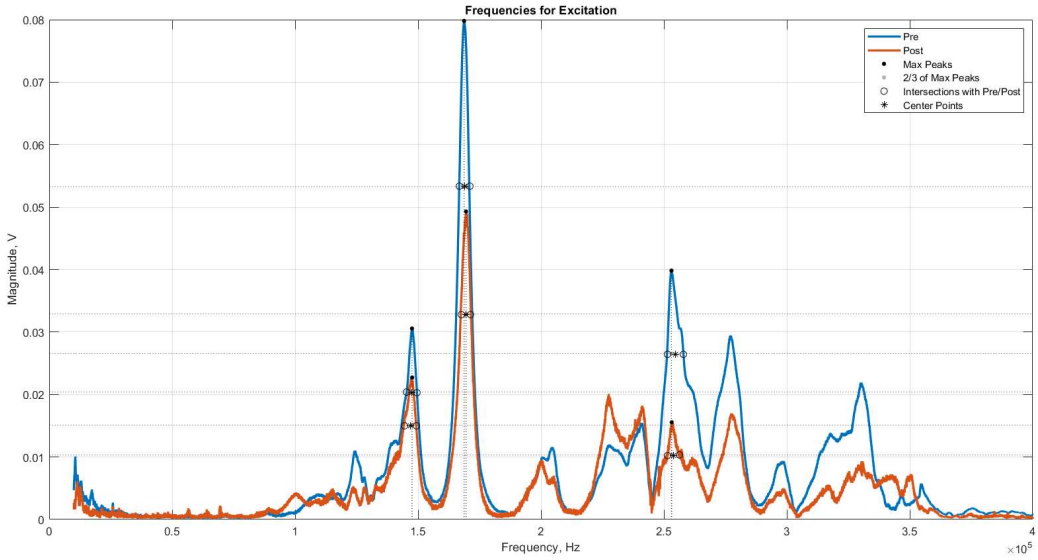

ALLIGATOR FEMUR 1 SPONGY 2

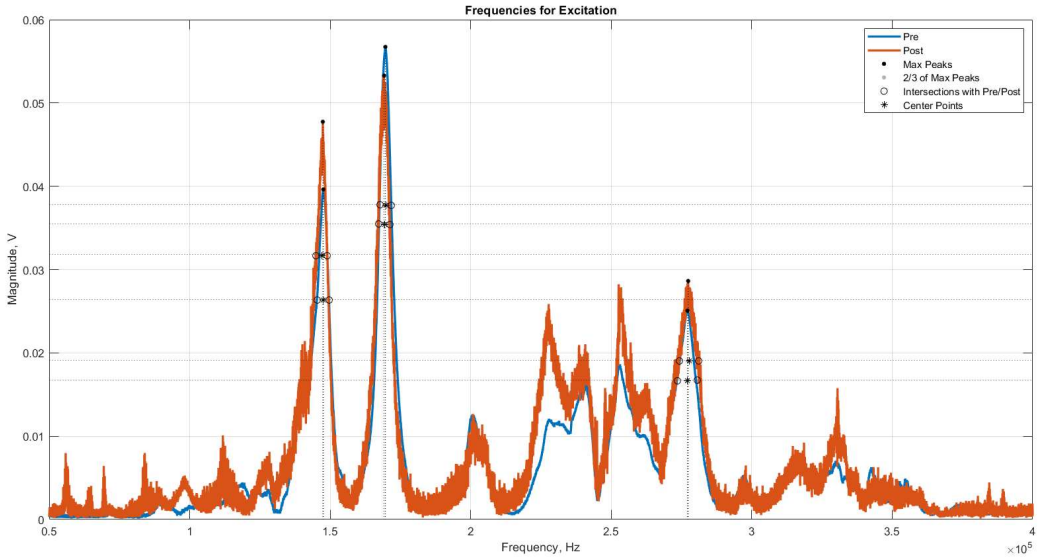

ALLIGATOR FEMUR 1 COMPACT 1

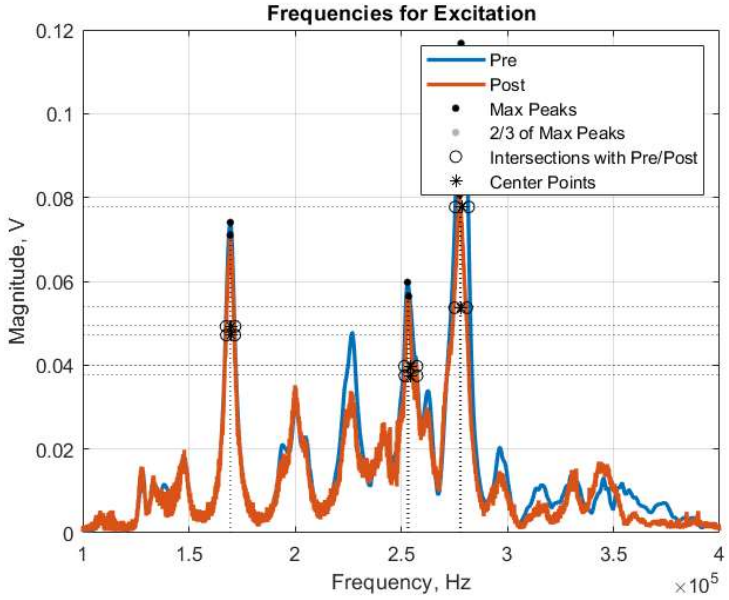

ALLIGATOR FEMUR 2 COMPACT 1

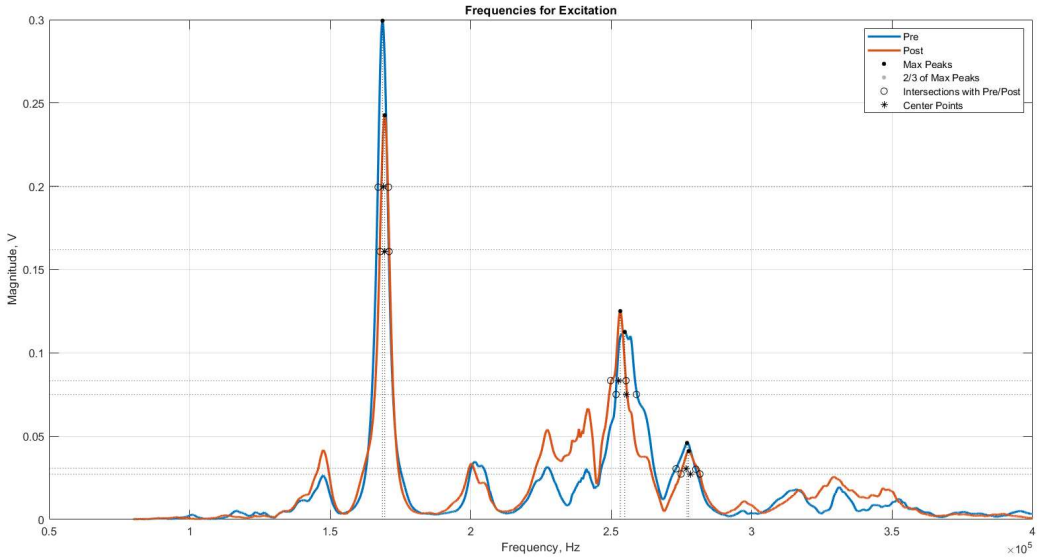

ALLIGATOR FEMUR 2 COMPACT 2

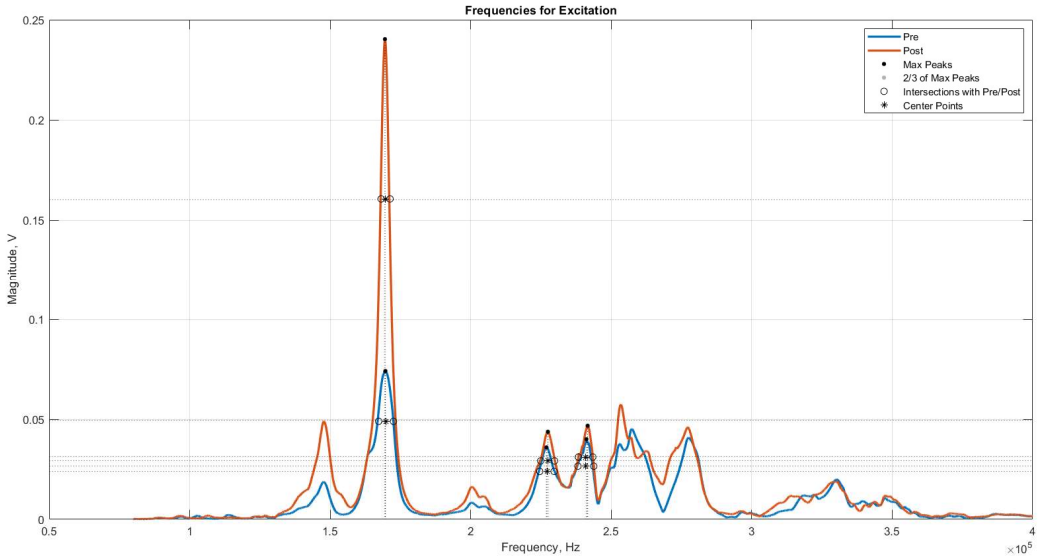

ALLIGATOR FEMUR 3 COMPACT 1

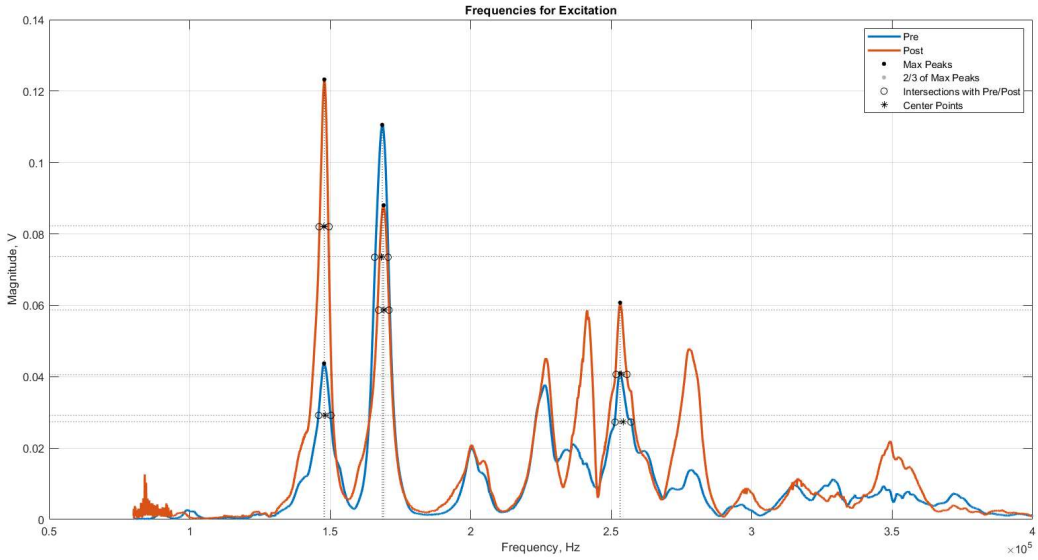

ALLIGATOR HUMERUS 1 SPONGY 1

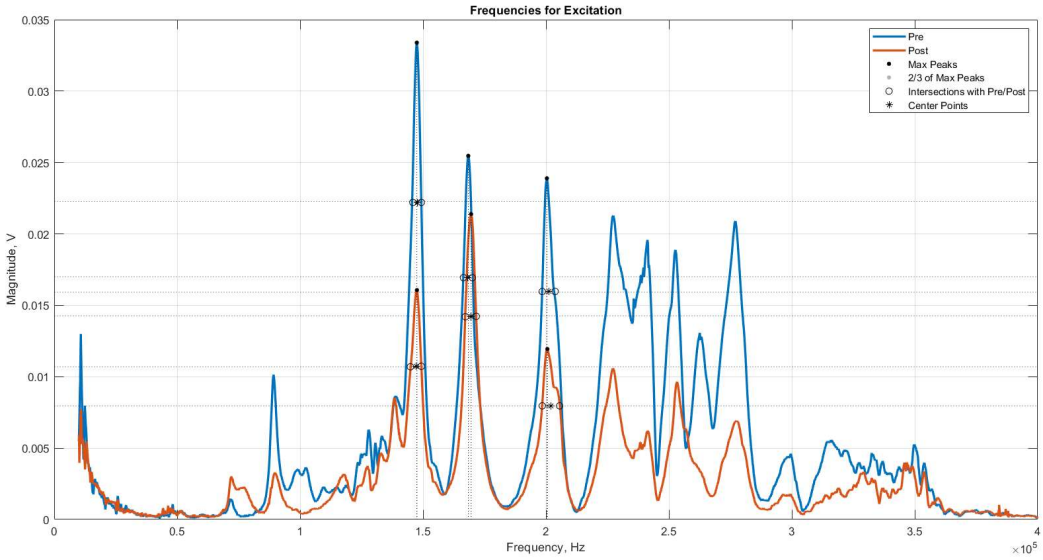

ALLIGATOR HUMERUS 2 SPONGY 1

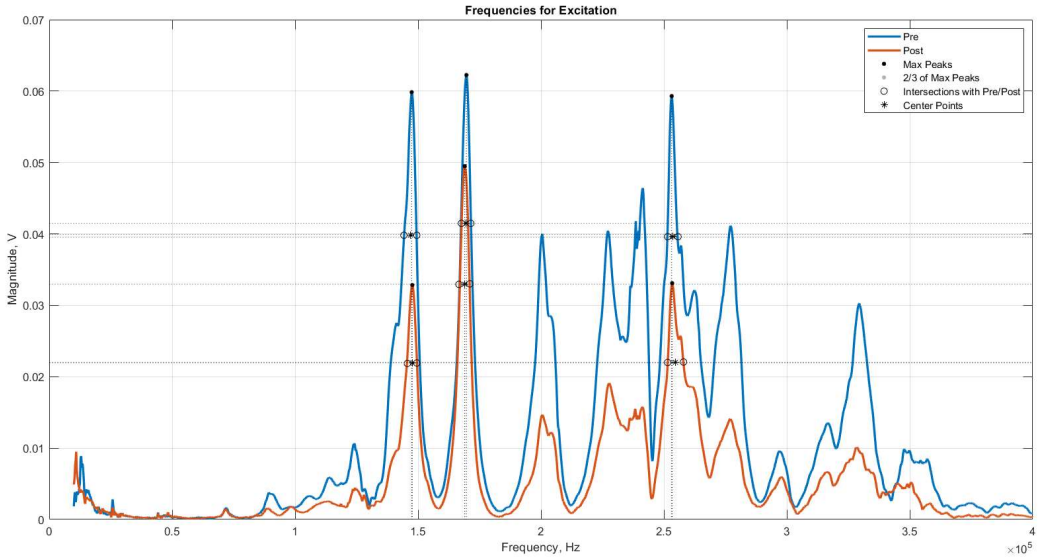

ALLIGATOR HUMERUS 2 SPONGY 2

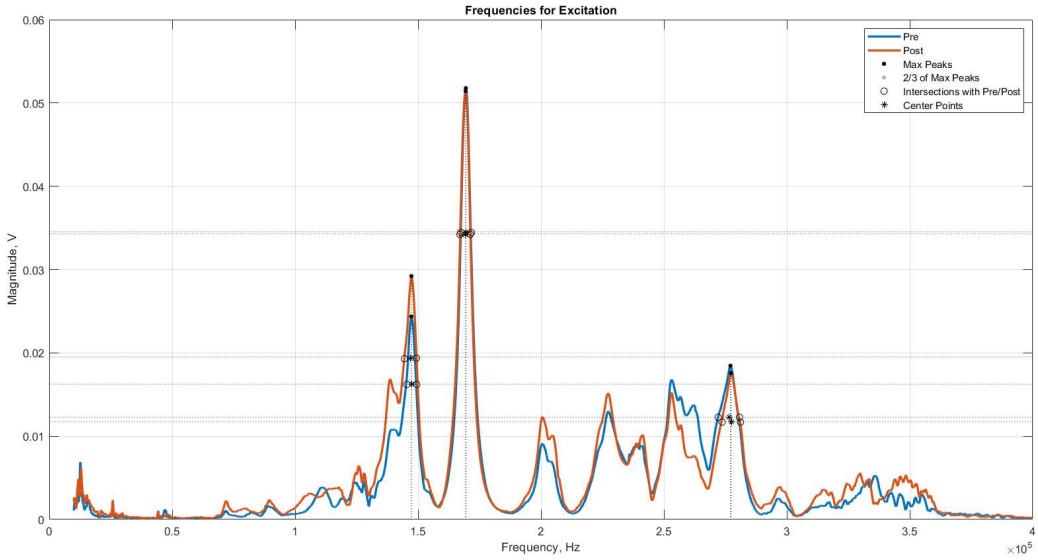

ALLIGATOR HUMERUS 2 COMPACT 1

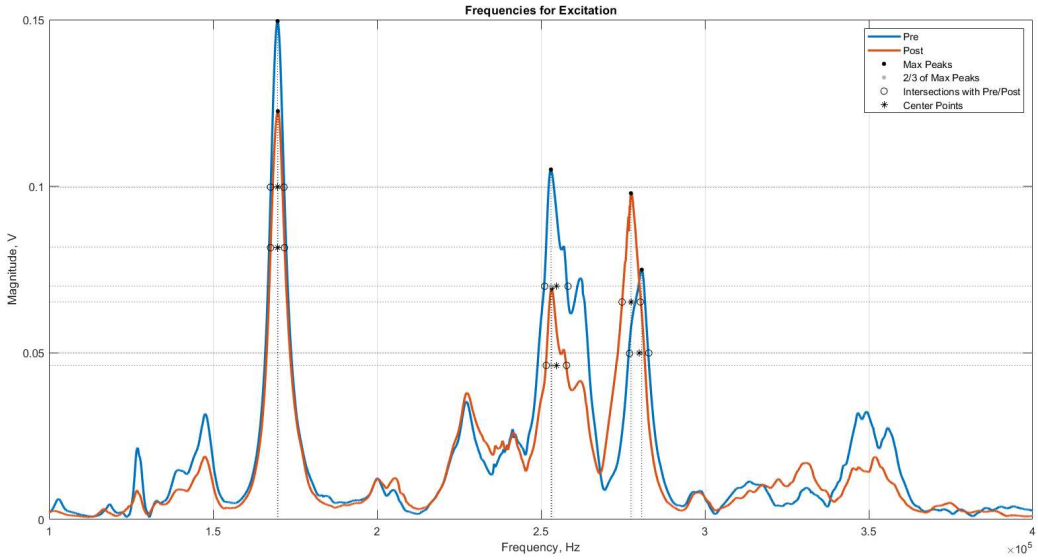

ALLIGATOR HUMERUS 2 COMPACT 2

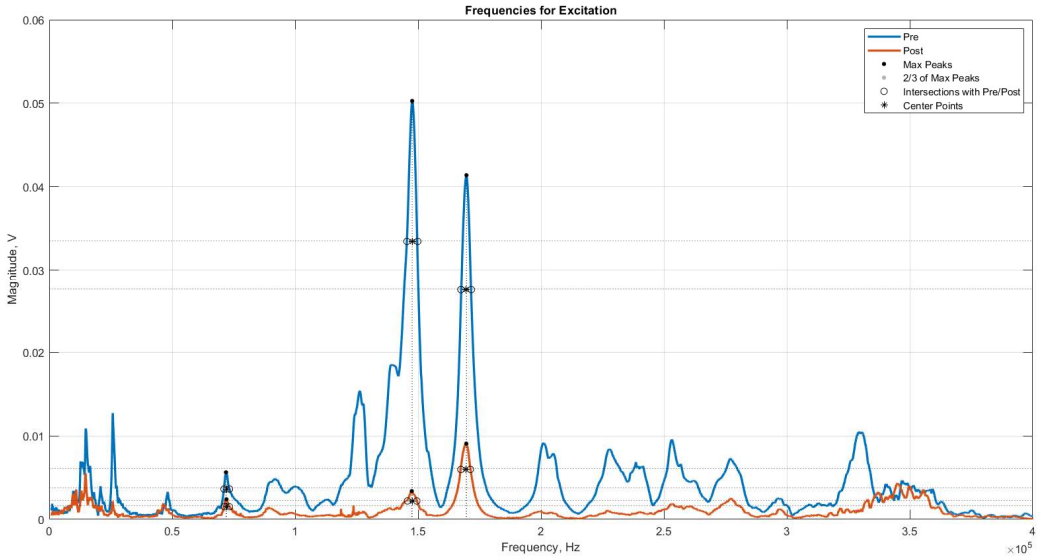

ALLIGATOR HUMERUS 3 SPONGY 1

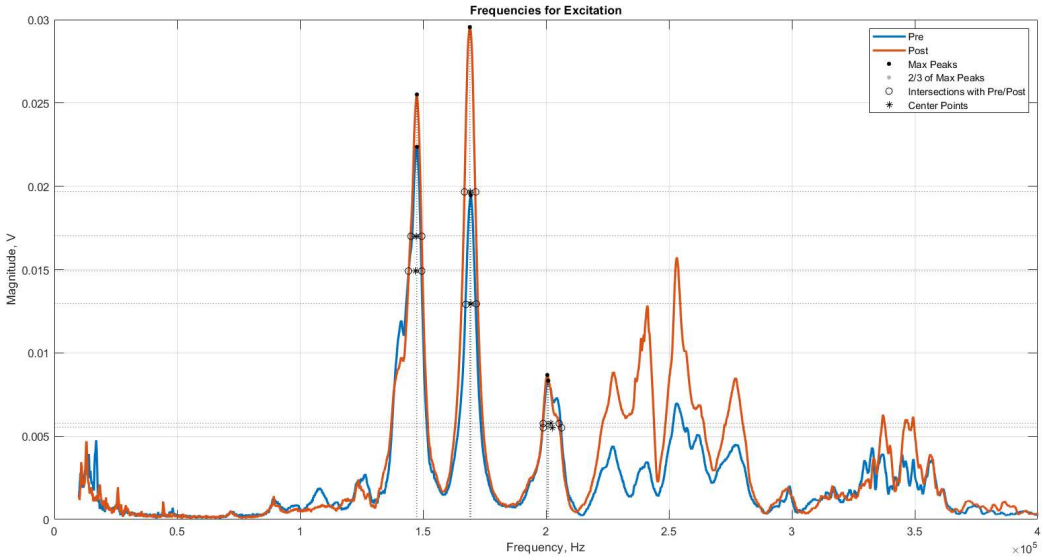

ALLIGATOR HUMERUS 3 COMPACT 1

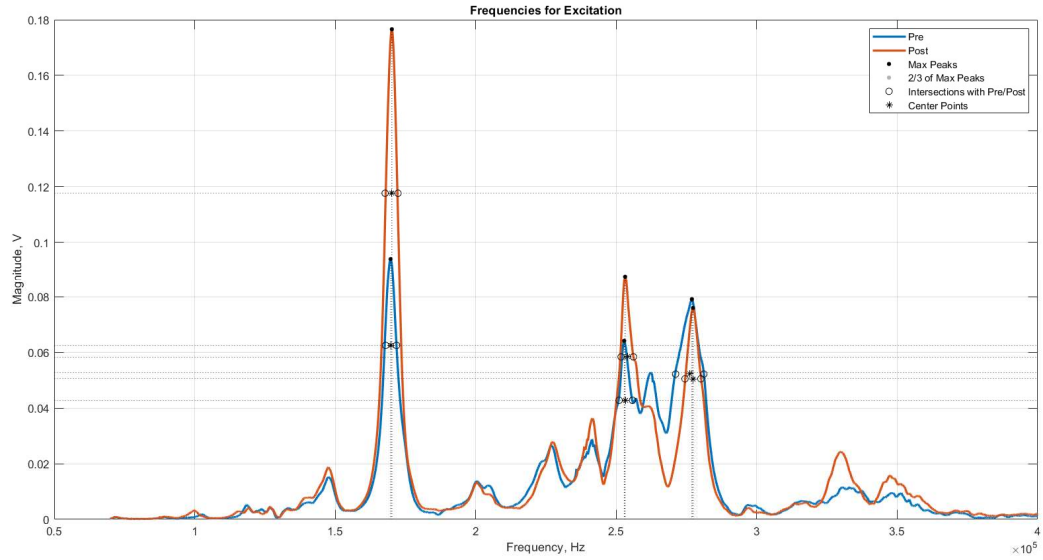

ALLIGATOR HUMERUS 3 COMPACT 2

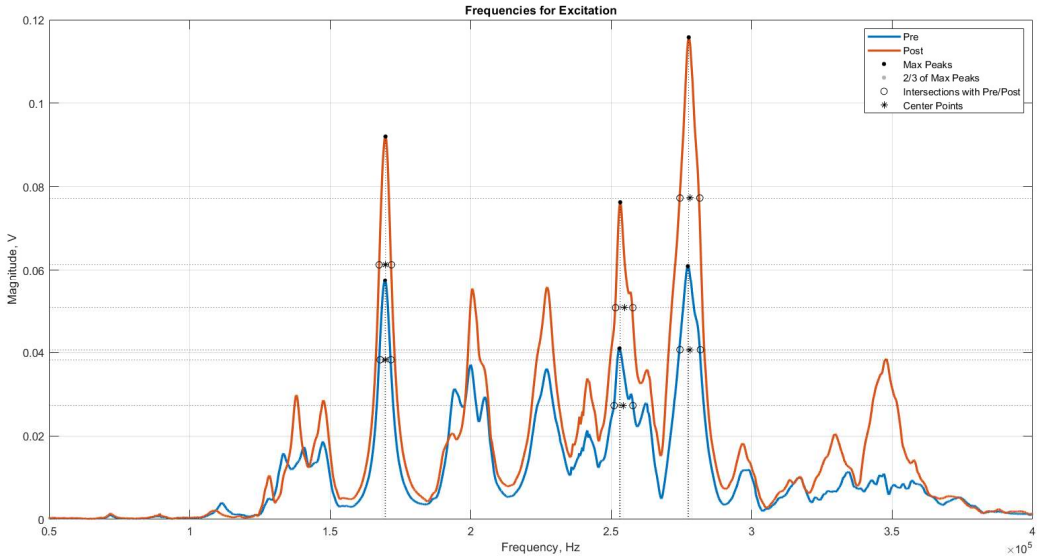

VITA

Parker Brewster

EDUCATION

University of Mississippi

BS in General Engineering, Minor in Chemistry and Biology **May 2020**

M.S. in Engineering Science (Mechanical and Biomedical) **GPA: 3.96, August 2022**

Ph.D. In Engineering Science (Chemical and Biomedical) **May 2025**

Foundation for Advanced Education in the Sciences

Excellence in Preclinical Innovation (Certificate) **May 2021**

EXPERIENCE

Founder and CEO, Innovative Heart Technologies, LLC. **February 2021 - Current**

- Designed medical device(s) that remove(s) arterial plaque
- Built the company, filed for provisional patent, won pitch competitions, and participated in accelerators
- Created custom website, designed and executed complex simulations, etc.

Graduate Student Researcher, University of Mississippi **May 2022 - Current**

- Worked on drug delivery innovation
- Assisted in the translation of innovation

Graduate Research Fellow, NIH (NCATS) **April 2021 - Current**

- Worked with industry titans on developing valuable machine learning code
- Presented and defended numerous posters
- Designed algorithms meant to predict bioactivity and efficacy of compounds

Graduate Student Researcher, University of Mississippi **May 2020 - August 2022**

- Built simulations and applications for predicting satellite's responses to physical stimuli
- Built simulations predicting thermal cycling of LEO satellites
- Executed research in the realm of thermal cycling and RUS (satellite components and bone)

Graduate Student Researcher, UAB (Radiology) **August 2020 - Current**

- Trained A.I. to predict outcomes based on CT scan measurements
- Created new means by which to make health care predictions and suggestions

Undergraduate Student Researcher, UoM (Pharm. and Biochem.) **September 2016 - May 2020**

- Worked in Pharmacognosy lab under Dr. Cole Stevens
- Served as lab leader in Dr. Wadkin's cancer research lab
- Built strong foundation of knowledge in wet labs and bacterial research (Defended posters)

ACTIVITIES and HONORS

Full-ride Scholarship, University of Mississippi **August 2016 - May 2020**

- Academic merit (36 ACT superscore), Engineering Supplemental Scholarship, etc.

Who's Who, University of Mississippi **2020 Academic Year**

Founder of Biomedical Think-Tank, University of Mississippi **May 2021 - Current**

- Founded and led inter-departmental club designed to inspire biomedical innovation

Mid-South Business Model Competition, National Competition **November 2021**

- Winner of 1st place and $10,000 for pitching my medical device and its business model

Undergraduate Researcher of the Year, University of Mississippi **May 2020**

- An award given for my contributions to undergraduate research

Founding Member of Effective Altruism, University of Mississippi **September 2019**

- Founder of club dedicated to effectively giving back to the community

NIH Presentation Finalist, National Institute of Health **August 2021**

- Honor received for research presentation/defense

SURE Program, University of Mississippi Medical Center **May 2016 – September 2016**

- Highly competitive summer research program
- Researched, presented, and defended research in both cardiology and radiology

SKILLS

SOLIDWORKS*(P)(C)(W)*, FDM & SLA 3D Printing*(P)(C)(W)*, Regulatory Pathway*(P)(C)(W)*, MATLAB*(P)(C)(W)*, Microcontrollers*(W)(C),* AutoCAD*(C)(W),* LabView*(P)(C)(W)*, Raspberry Pi*(C),* Wet Lab*(P)(C)(W),* Python*(P)(C)(W)*, Machine Learning*(P)(C)(W)*, KNIME*(P)(C)(W)*, Scikit-Learn*(P)(C)(W)*, Preclinical Innovation*(P)(C)(W)* ****Certified by NIH****

(P)- Proficient (C) – Class Experience (W) – Work or Project Experience